

Journal: ACP

MS No.: acp-2018-784

Title: Receptor modelling of both particle composition and size distribution from a background site in London, UK – the two step approach

Author(s): David C. S. Beddows and Roy M. Harrison

RESPONSE TO REVIEWERS

REVIEWER #1

General comment: The paper regards the description of a two-step approach for performing source apportionment using the PMF receptor model and an input composed by variables having different measurement units. The approach has elements of originality and potentially several applications. The topic is interesting considering that source apportionment is a major topic in nowadays research and the possibility to use an approach that use input variables having heterogeneous measurement units is certainly appealing. I also believe that the topic is suitable for the Journal and the paper generally well written and understandable. However, I found that some aspects are not completely clear (see my specific comments) and the paper need a revision before publication.

RESPONSE: We thank the reviewer for these positive overall remarks.

Specific comments:

Lines 59-62. This sentence is not completely true and I would suggest to modify it. This happens only if number size distributions are mixed with chemical composition (in mass), however, there are examples in which size-segregated chemical composition is used in PMF analysis to obtain quantitative evaluation of size distribution of sources (see for example Contini et al., 2014 Science of the Total Environment 472, 248–261 and references therein).

RESPONSE: Text has been added to this effect, saying that by careful experimental design the issue of datasets with heterogeneous units can be avoided, for example using a Cascade Impactor to measure size-fractionated chemical PM mass composition rather than two measurements: one for particle number size and the other for total PM mass.

Lines 140-141. Better to write 16-604 nm (like in line 149) because two decimal digits for size is an illusory precision.

RESPONSE: Correction made.

Lines 159-161. The conversion of mass difference in PNO.6-10 is likely quite uncertain. Some details should be given because I believe that some assumptions have been done regarding size distribution in the range 0.6-10 micron and the result of the conversion would be strongly influenced by these assumptions. A comment on this aspect is needed.

RESPONSE: This section has been re-written to include more details and a statement added that a large uncertainty is applied to this measurement so as not to influence the final results.

Lines 312-314. This could happen because nanoparticles have a limited mass to influence significantly PM10 mass composition, however, it could be different if NSD are mixed with PM1 chemical composition for example. A comment on this aspect would be useful.

RESPONSE: Within the context of response to comments on lines 59-62, we have commented on this to say that with a different measurement, PM₁, the NSD data would give a better overlap. However, having said this, PN measurements have a sensitivity bias towards the smaller nucleation particles whereas PM measurements have a bias towards the more coarse particles.

There is a particular reason for using PMF2 and not the more advanced PMF5 that is becoming the standard version of source apportionment with PMF?

RESPONSE: PMF2 is not version 2 of the US EPA PMF. PMF2 is the ordinary 2-way factor analysis as opposed to the 3-way factor analysis PMF3 or ME-2 for solving arbitrary (quasi) multilinear models. This has been clarified in the Experimental part of the text.

Lines 215-216. How much is it the X value chosen? This should likely be reported for completeness.

RESPONSE: We have added this information, which says that once fitted the NSD data have a relative uncertainty of 4-5%.

Line 259. I believe that the number of factors is six rather than seven.

RESPONSE: Yes, the correction has been made.

Lines 358-360. Looking at figures 4 and S3, it seems that the marine source is dominated by nanoparticles. Considering that this is a source generally made of coarse particles, and also authors mention this aspect, this result appears unusual and some discussion and explanations are needed.

RESPONSE: This apparent contradiction has already been addressed in Beddows et al. (2015) in the five-factor solution from the combined composition–NSD data set. In this, a factor which can be clearly assigned on the basis of its chemical association is that described as aged marine. This explains a large proportion of the variation in Na, Mg and Cl but shows a NSD with many features similar to that of the traffic factor, with which it has rather little in common chemically. Since the aged marine mass mode is expected to be in the super-micrometre region and hence well beyond that measured in the NSD data set, it seems likely that the size distribution associated is simply a reflection of other sources influencing air masses rich in marine particles. The main point to take away is that we get the same solution using the 2-step approach.

Minor comments:

Lines 148. “spherical”

RESPONSE: Yes, the correction has been made.

Line 351. “there is...” The source “NET and crustal” is reported in the text but repeated in the figures as “NET and coarse”. I would suggest to use “NET and crustal” in all the paper that is more understandable and appropriate.

RESPONSE: Yes, the correction has been made to be consistent with our original work in Beddows et al. (2015).

Title Section 3.4. Why hidden?

RESPONSE: The work hidden has been replaced by unresolved. It was not resolved until a 7 factor solution was chosen using an FKEY matrix (as specified in Figure 3 with 6 x 6 zero diagonal FKEY matrix augmented with an 7th column and 7th row of zero entries).

Moreover, this section is dedicated to several factors...what is the hidden one the nucleation? An explanation or a change of the title is needed.

RESPONSE: Extra explanation is given.

What is the meaning of the “*” reported in figures 4 and 5?

RESPONSE: These have been removed.

REVIEWER #3

The manuscript has several elements of originality (to my knowledge, no similar methods have been already published) and directly hits a very controversial and up-to-date topic in the atmospheric sciences. Nowadays, source apportionment by PMF is amply used in both routine monitoring and research studies. Although most of them use “one-kind” variables (mostly PM chemical speciation data), an increasingly high number of studies (just a few have been cited in the manuscript, but the list should be improved) use variables with multiple units. Since the large number of available air quality measurement techniques, the merging of dataset(s) with different units is a suitable (and proven) way to better resolve the PMF source

profiles and to detect unresolved sources. Essentially, additional variables may help in better detecting the edges.

RESPONSE: We thank the reviewer for this positive perspective on the work.

Under this view, a recent paper (Emami and Hopke, *Chemometr. Intell. Lab. 162* (2017) 198–202, which findings are unfortunately not considered in this manuscript), showed the effect of adding variables with different units to decrease the rotational ambiguity of PMF solutions.

RESPONSE: This paper has now been cited.

Thus, the topic is suitable for the journal ACP. However, the manuscript needs revisions before to be accepted for publication. Major points. Essentially, the rationale behind the whole manuscript is based on the statement reported in lines 59-62: “However, while combining, for example, particle chemical composition and size distribution data in a single PMF analysis may assist source resolution, it does not allow quantitative attribution of either particle mass or particle number to the source factors.”. Later, the authors also presented a case study where they mixed variables with different units without giving quantitative results. Even if one can agree with this statement, the authors have not exhaustively explained it. Since this is a methodological manuscript, I strongly encourage the authors to better support these statements.

RESPONSE: The comment regarding the unapportioned factor analysis of data with heterogeneous units from the supporting output of Beddows et al. (2015), is referred to in Section 3.2 entitled 2-Step PMF-LR Analysis. We have expanded this section of text to report more clearly, what was carried out in the supporting study.

Another major weakness of this manuscript is the lack of sufficient details on the PMF analyses. This point can be easily solved by the authors, who have an extended experience with PMF analysis. This manuscript presents a new approach, so particular care should be given to details so that anyone can easily reproduce what the authors did (and test with their own data). However, details of the PMF are generally missing or they are reported in the companion paper (Beddows et al., 2015).

- For example, the authors should describe the method(s) used to compute the uncertainties in the 1st step (including PNO.6-10, see next point).

RESPONSE: This section has been rewritten to give more detail.

- Also, the authors should report how the raw data have been handled (if any correction was done) and the number of variables and cases inputted into the models. For example, they should report the outliers detection and how they managed the missing values (SMPS sampled every 15 min, what is the minimum number of 15 min records to have a valid 1-hour NSD value?).

RESPONSE: The details of the SMPS setup are now in Table S1 and a note is added to say that the raw data was quality assured by the National Physical Laboratory (NPL), and to see Beccaceci et al. (2013a,b) for an extensive report on how the data was collected. Furthermore, we addressed these points by carrying forward the descriptions in Beddows et al. (2015) of how the PM₁₀ data was collected and prepared for this study.

In addition, since the Q values are used (lines 199-203 and 215-216), they should be reported as well. Furthermore, it is unknown if the authors dealt with the rotational ambiguity of the models.

RESPONSE: This is addressed in the response to P. Paatero’s comments.

The authors used R to “optimize” X to have $Q/Q_{theory} \sim 1$. More details should be reported. In particular, what does “ ~ 1 ” mean? It can be every number, but having it from 0.5 to 1.5 or from 0.99 to 1.01 makes a big difference. Please explain.

RESPONSE: We have set a criterion of within 1 ± 0.02 .

Basic information on the PMF set-up is important to report. This information will allow the reader to completely understand what the authors did and (possibly) to reply the methods. It would be useful to

have a quick overview of such details in the main text with the deepest description in the supplementary information.

RESPONSE: This point has been addressed within the rewritten mathematical description of the PMF analysis.

Another unclear point is related to the “proxy-data” used to assess the PN0.6-10 variable. This is an artificial variable: it was not directly measured, but it was computed on the basis of two (three?) main assumptions: (i) particles are assumed to be spherical, and (ii) particles have fixed density. But it is not completely clear if the density is assumed constant over the time or over the whole (16-604 nm) size spectra (or both, as it should be). The authors used a density of 2 g/cm³ over all the study period, but they report a 1.8-2.5 g/cm³ range for an urban background aerosol. Consequently, the PN0.6-10 variable will be affected by a large uncertainty that cannot be well assessed. I suggest to add more details and provide an estimate of the uncertainty of this new variable.

RESPONSE: Clarification of this has been made by adding a fuller and more mathematical description to explain how the proxy variable is calculated and how the density value is used.

This latter point raises another question. Why the authors did not plan to also use an APS to complete the size range to 10 μm? One can argue that the sampling campaign was not planned to have an APS included (or the merging of SMPS and APS was unreliable). However, my opinion is that this point should be at least mentioned in the text, so colleagues who want to pursue the same approach are advised on the possible use of wide range particle size spectra.

RESPONSE: We have added this point to a list of alternative approaches to using the proxy-data at the end of Section 2.2.

Minor comments:

Line 103. Missing bracket “)”

RESPONSE: Corrected.

Subsection 2.1: Please add more details on the SMPS set-up. For example, sheath and sample flows, the status of the CPC and electrostatic classifier (serviced, calibrated?), the type of neutralizer (X-ray, 85Kr?), software/algorithm used for the data inversion (or version of the AIM software), use of multiple charge and/or diffusion loss corrections, etc. These details need to be added as supplementary information.

RESPONSE: This has been added in Table S1, although it does seem like too much information for what the referee correctly identifies as a PMF methodology paper; it is not a data collection paper.

Line 138: 1 4 hour -> 15 min

RESPONSE: Change made although this is considered to be a personal preference.

There are two equations numbered as (3), see pages 11 and 12. This should be fixed, as most of the discussion on the method refers to these equations.

RESPONSE: Correction made.

Figure 3 can be easily moved to the supplementary material file.

RESPONSE: Figure moved.

Figure 4. NET & coarse should be NET & crustal.

RESPONSE: Correction made.

Figure 6. Once printed, the labels and axes of the single plots will be likely unreadable. Please increase the font size and (if possible) please uniform the font style and size among the figures. Also, it is advisable to use a color scale that is also easily readable when the paper is printed with a black and white printer.

RESPONSE: We have increased the font size at the expense of the size of the plots which has improved the readability of the text in these plots. However, we have not found a palette which

looks good in colour and preserves the information in black and white. All we can suggest is that a grey scale is used for the option of black and white printing.

Figure 6 shows polarplots and polarannuli. These “openair” analyses are commonly reported in air quality studies and are very helpful to better interpret the data. However, a quick overview of the information provided by these two plots should be briefly reported into the materials and methods section.

RESPONSE: General descriptions of polarPlot and polarAnnulus have been added to the Methods Section.

REVIEWER #4

The paper by Beddows et al. described a two-step source apportionment methodology on a combined database of both PM mass and number size distribution measurements carried out in London. A previous source apportionment study using the same database had been reported by Beddows et al. (2015). Thus, the novelty of this study could be represented by the methodology development. The topic is interesting, and the methodology would be useful in deal with mixing data types as input in PMF, which provide a better defined source factor and better fit diagnostics compared to when non-combined data were used. However, I found that some aspects are not clear and improvements should be made before the work be published in ACP.

RESPONSE: We thank the referee, and we welcome the opportunity to provide greater clarity.

Major comments:

1. The motivation of this study is to clarify the source contribution when a combined database was used in PMF. As the authors state, the combined PM chemical composition and size distribution data in a single PMF analysis could not allow quantitative attribution of either particle mass or particle number to the source factors. However, one could calculate the source contributions either by PM mass or by NSD base on the output results of PMF. The following reference is an example described the source contribution using combined database in PMF. Please clarify this item. Sowlat et al., 2016. Source apportionment of ambient particle number concentrations in central Los Angeles using positive matrix factorization (PMF). *Atmos. Chem. Phys.*, 16, 4849-4866,

RESPONSE: We do calculate the source contributions either by PM mass or by NSD based on the process of using output from the PMF results in Beddows et al. (2015). Those results are carried through into this work, so we are already carrying out a 1-step analysis resulting in an apportionment. To address this oversight of the referee, we have added a line to Figure 2 saying “[The PMF analyses of Beddows et al. (2015) are considered as Step 1].” We have also added a table of apportionment values from Beddows et al. (2015) into Figure 1 as an insert showing the apportionment of the factors, and the reference to Sowlat et al. (2016) which is very similar to Harrison et al. (2010), which reports PMF of merged SMPS-APS data and chemical and meteorological data.

2. The two-step PMF-PMF method is new but the results maybe questionable. The G1 time series from the PMF analysis of PM10 chemical composition (Step One) could be considered as a constraint in Step Two, which means that six factors identified by PM mass was also applied to NSD. I think this is why the results from two step PMF-PMF method was different from results using combined dataset of PM and NSD in PMF reported by Beddows et al. (2015).

RESPONSE: The reviewer is correct in this interpretation.

Thus, what about the results if using the G1 time series from the PMF analysis of NSD as step one? Please clarify this item.

RESPONSE: The aim here is to assign a NSD description to the PM₁₀ mass sources, so we are not sure why we would consider a 1-step PMF analysis of the combined G1 + NSD data set without applying an ‘FKEY constraint’. When removing the FKEY constraint, there is no clear separation of the G1 scores and we can no longer match the NSD of the resulting factors to the original source. Instead we have to introduce new descriptions based on the 6 factor names: Diffuse Urban; Marine; Secondary; NET / Coarse; Fuel Oil and Traffic. Furthermore, a conclusion from Beddows et al. (2015) was that a better result was obtained when analysing the datasets

separately. This work continues with this recommendation by heavily biasing the analysis to the data analysed in Step 1.

Specific comments:

1. Line 157-160. The particle number greater than 600nm is calculated from the difference between PM10 and PM0.6 estimated from SMPS. Except PM0.6-10, particle density, particle shape (spherical) and size distribution should be known when calculating the PN0.6-10. Please provide more description about the calculation process.

RESPONSE: This point has been addressed in line with the comment of Referee #1.

2. Line 355-356. Why the secondary factor be expected to be strongest at night? 3. Line 362-363. These are not Fig. 7 in the text.

RESPONSE: Typo: Figure 7 is Figure 6. This has been corrected. Furthermore, the secondary factor is expected to be stronger at night when compared to the secondary NSD factor derived in Beddows et al. (2015). In Beddows et al. (2015), both the secondary component derived from the PM₁₀ and NSD analysis are strongest at night, and in particular, the PM₁₀ secondary factor has a strong nitrate component which does grow to a maximum during the night due to reduced volatility of ammonium nitrate. Clarification has been given.

REFeree: P. PAATERO pentti.paatero86@gmail.com

This manuscript deals with PMF analyses of "combined" data matrices such as [X Z] where X contains elemental composition profiles of aerosol samples and Z contains aerosol number size distributions measured simultaneously with composition profiles. This is an important problem that occurs often in modern aerosol research. There are specific problems in this task; these problems have not been studied in depth in literature so far. This manuscript studies one specific combined data matrix and reports a PMF model for this matrix. Thus the ms might deserve publication despite of certain serious problems. These problems are in part related to misunderstandings found in earlier papers that discuss this same topic. For this reason, the present review contains a lengthy general discussion of the task of modeling combined matrices. The specific questions regarding this ms are based on this general discussion. The ms might also be suitable for publication in the sister Journal AMT, Atmospheric Measurement Techniques. My personal view is slightly in favour of AMT. However, both ACP and AMT seem possible, and this review considers publication in either Journal. The structure of this review is as follows:

RESPONSE: We recognise the immense contribution made by Professor Paatero to this field, and thank him for the critical insights which he provides.

=====

Recommendations

Notation used in this review

Background

Common mode errors

Joint matrices containing different units

Discussion of the manuscript

Two-stage PMF model vs. customary PMF model

The hidden factor, aka Nucleation factor

Miscellaneous

Recommendations

There are very many problems of different kinds in this manuscript. For this reason, I hesitantly recommend that this ms should NOT be published by ACP or AMT. However, if it is desired to publish this ms because of the importance of the problem, then a thorough rewriting of the text and mathematical details must be undertaken. I recommend that the following enhancements be performed: There has apparently been lack of communication between the person(s) who did the actual computations and those who wrote the paper.

RESPONSE: This first author is responsible for both the computation and the manuscript and we have endeavoured to follow these recommendations to avoid the appearance that an unnamed contributor has been involved. The paper has been extensively revised in response to the comments of all four reviewers.

For this reason, the mathematical description is erratic, chaotic and impossible to understand or replicate. In order to create an accurate description, the person(s) who did the computations should be included in the group of authors. Without such help, it may not be possible to achieve a satisfactory mathematical description of what was done. The entire mathematical discussion about problems attributed to PMF analysis of joint matrices containing different units is erroneous, based on a widespread misunderstanding. This discussion must be rewritten according to suggestions given below. It might be good to include in the author group somebody familiar with the quantitative mathematical structure of the PMF model.

RESPONSE: Thank you for highlighting this misunderstanding which we have addressed in the revised manuscript.

In particular, it seems that lines 79,80 are not based on quantitative understanding of the model. These lines, and other similar sentences, must be removed. Much of Conclusions must be rewritten so that the claims against using variables with different dimensions/units are replaced by opposite sentences stating e.g. that a joint analysis of matrices of variables with different dimensions/units is not harmed by these differences but unfortunately the opposite was believed to be true when the work was carried out.

RESPONSE: This correction has been carried out.

The mathematical description of what was done must be totally rewritten so that systematic matrix-form notation is used. Equations must be corrected and written in correct notation, using correct terminology and correct numbering. Details of PMF modeling must be reported, such as dimensions of matrices, used parameters such as uncertainties of data values, robust/nonrobust, obtained Q values, numbers of observed outliers, unique or multiple minima, and so on.

RESPONSE: This has been corrected following the guidance of all the other referees.

Rotational questions are an ever-present problem in factor analytic modeling, independently of what programs are used. It is alarming that the word "rotation" does not occur in this manuscript. Pay attention to rotational questions. There are certain weaknesses in the plan of this work, such as assuming that the rotational status of the original PMF model of X was correct or best possible (see below). These weaknesses cannot be corrected in an enhanced ms but they should be briefly discussed. This is important because otherwise, colleagues following the example of this work will feel the need to replicate everything that was done here, being unaware that some details may not have been optimal.

RESPONSE: Rotations are now briefly discussed.

Enhance figure captions so that readers do not need to guess what is shown. Have the enhanced ms proofread by colleagues. Check also the references. This ms illustrates, once again, how difficult it is to find ones own mistakes and typos.

RESPONSE: Enhancements of figure captions have been carried out.

Notation used in this review

The notation "[X Z]" indicates here attached or joined matrices, i.e. placing X and Z side by side so that they form one larger matrix. The notations G(X) and F(X) will indicate factor matrices (G and F) obtained from an individual PMF model of X only, and similarly G(Z) and F(Z) for Z only. The left and right parts of F, when modeling [X Z], are denoted by F[Xz] and F[xZ]. Q(X) and Q(Z) indicate Q values from separate analyzes of X and Z. Similarly, Q[Xz] and Q[xZ] denote Q sums computed over elements of X and over elements of Z in the joint analysis of [X Z]. Hence, $Q[X Z] = Q[Xz] + Q[xZ]$. Total weight of X means the sum of squares of X_{ij}/s_{ij} over X, where s_{ij} is the uncertainty assumed for X_{ij} . If both X and Z are equally important, and if X and Z are of different sizes, all s_{ij} reported for the larger matrix should be increased so that total weights of X and Z become approximately equal. This implies a deviation from the general principle of determining weights from std-dev of values.

RESPONSE: An amended notation as suggested has now been implemented.

Background

Before examining this manuscript in detail, it is necessary to discuss the model that it tries to solve and the problems that make this task difficult. It is known that PMF of combined matrices often leads to disappointing results, such that some factors only (or mainly) fit X while other factors only/mainly fit Z. Such result is worthless in cases where X and Z are caused by the same emission sources whose emission profiles should be determined for X and Z. It is important to realize what advantages may be expected from the joint analysis of X and Z. Three Cases are possible: PMF models computed separately for X and for Z may be valid and rotationally unique for (A) both X and Z, (B) one of them (for X, say), or (C) neither one of them.

Case A: If individually computed factors $G(X)$ and $G(Z)$ are practically identical, then a straight-forward joint model is successful for this case. Then $G_{[X Z]} = G(X) = G(Z)$. If $G(X)$ and $G(Z)$ are significantly different, however, then the joint model will fail, producing too large residual values and hence too large Q. Such result might be caused e.g. by "common-mode errors" (see below) in X and/or in Z.

Case B: Now a joint model should be specified so that total weight (see Notations, above) of better-analyzed matrix X is significantly higher than total weight of Z. Then X will "drive the model", and $G_{[X Z]}$ will be approximately equal to $G(X)$. If a reasonable $Q[xZ]$ is obtained, then it indicates that X and Z are compatible, i.e. a joint PMF model is meaningful. Larger Z residuals and larger $Q[xZ]$ would be obtained e.g. if X and Z do not have common sources or if there are common-mode errors. Then the joint PMF model is not meaningful for the chosen number of factors.

Case C: individual PMF models of both X and Z contain rotational ambiguity and/or other problems such as unidentifiable factors or missing factors. In this case, the approach of Case B cannot be used because the obtained ambiguous rotation, based mostly on X, may not be the best rotation for fitting Z. Ideally, equal total weights should be applied on X and Z, hoping that the best rotation for fitting both will be obtained when rotational information from Z is combined with information from X. Experience shows that quite often, such modeling fails. Few, if any, studies have been made about the reasons of such failures. It must be stressed that these failures must not be ascribed to "different units used in X and Z" (see below). As a first remedy, one might inspect the residuals in order to see if common mode errors are visible. Such errors might be corrected by hand, or by using an enhanced PMF model that automatically corrects for common mode errors. One might also inspect individual variables in order to see if only few variables are causing incompatibility of X and Z. Such variables might be downweighted in order to obtain a better overall model. Of course, one must also consider the possibility that in addition to their joint sources, X and Z may also have one or several unique sources. An enhanced PMF model may be developed for analysing such joint matrices containing common and non-common sources.

Summary of Case C: too little is known about reasons why this case fails. Well documented case studies are needed. Singular value decompositions of G matrices computed for X, Z, and $[X Z]$ may be useful for demonstrating the root of the problem. Reliable remedies may only be suggested when more is known about the reasons for failures in joint PMF modeling.

RESPONSE: An account of cases B and C has been added to the paper.

Common mode errors

Certain problems in measurements will cause so-called "common mode" errors. E.g. an error in air volume control in an aerosol sampler, when measuring sample i, causes that all aerosol concentrations on row i of X will change by the same fractional amount. Such common mode deviation does not contribute to residuals in customary PMF analysis of such aerosol data. Instead, common mode disturbance of sample i will change all elements of row i of matrix G. In a combined matrix, the other part Z is often measured using another instrument. Then Z may have its own common mode errors, different than those of X. In a joint analysis of X and Z, two independent sets of common mode errors will cause increased residuals when factors are common to X and Z. It appears highly probable that such common mode errors are an important

reason for those PMF results where individual factors tend to fit either X or Z but not both. Joint matrices containing different units This ms claims that quantitative PMF modeling of a joint matrix [X Z] is not possible if variables in X and Z are measured in different units, such as mass concentration (expressed in mass/airvolume) and particle number concentration (expressed in particles/airvolume). These claims are based on a widespread misunderstanding, as explained in this section. Customary aerosol PMF models are often scaled so that the sum of all elements in each row of matrix F equals unity. Then factor element F_{pj} indicates the fraction of species j in profile of source p. With joint matrices containing different units, summation over a row of F is not meaningful. The following workflow should be used instead in order to preserve the quantitative nature of the model: In PMF (or after PMF), scale factors so that the average of each column of G is scaled ("normalized") to unity. Then elements of F have the following quantitative meaning: F_{pj} indicates the average contribution of source p to observations in column j, both for species j in matrix X and for species j in Z. The average total amount of all aerosol species in source p is obtained by summing values F_{pj} over all species j in $F[Xz]$, i.e. in the part of F corresponding to aerosol matrix X. In this way, the customary interpretation of F_{pj} as fractions of total may be obtained "off-line" after PMF computations by dividing the F_{pj} values by their sums taken over $F[Xz]$. The ms also suggests that presence of other variables (Z) in PMF model somehow makes the model non-quantitative or unreliable: ms lines 79-80: there can be no confidence as to whether the sources are apportioned by units of number concentration (1/cm³) or any of the other units used in the auxiliary data. Units may be entirely ignored in PMF modeling if all variables are represented in same units. If different units are present in different columns of matrix X, then the following practice is followed: elements of factor matrix G are pure numbers. Elements in column j of factor matrix F carry the same dimension and unit as column j of data matrix X. In the present case, all elements of left part $F[Xz]$ of factor matrix F will be in mass/airvolume (same as X) while all elements of the right part $F[xZ]$ are in units of number concentration (1/cm³) (same as Z). There is no confusion regarding dimensions or units.

Disturbance of quantitative modeling of X by "other variables" in Z may only be present if Z variables make the fit of X extremely poor, so that $Q[Xz]$ increases to unacceptable levels in comparison to the original $Q(X)$. This can be seen from Eq. (1) which defines PMF model: all values in column j of X are fitted using F factor elements from column j of F only. The "other columns" in F, corresponding to "other variables" in Z, do not enter in the fit of any X variables. If $Q[Xz]$ remains normal, model of X remains quantitative even when Z is introduced in modeling. However, if introduction of Z requires that number of factors must be increased, then the two models are different. Then rotational uniqueness and interpretability of the joint model of [X Z] may well be better or worse in comparison to the original model of X only. On the other hand, $G(X)$ and $G[X Z]$ may appear significantly different even when all Q values are normal. In this sense, including Z may interfere with the fit of X although the new fit of X remains as quantitative (or better) than the original fit of X. Such effect depends on rotational ambiguity of the original PMF fit of X: when Z is introduced, it may "rotate" a rotationally ambiguous model of X so that Z obtains a better fit while $Q[Xz]$ does not increase from $Q(X)$ or increases a little. Such rotation may only occur if the original model of X is rotationally ambiguous, "non-quantitative". If such ambiguity is not understood by the scientist, it might appear that introduction of other variables "harms" the original model. In contrast, however, modifying the original model of X by a rotation is what is desired when using the joint model: both X and Z should be fitted as well as possible. This effect does not harm the quantitative nature of the model, as long as Q value of X does not grow too much. Summary of this section: if Q computed over X elements increases significantly when modeling [X Z] instead of X, this indicates that X and Z are not compatible (when assuming this number of factors). Then analysis of [X Z] should be rejected. In all other cases, the joint model of X is equally good or better than the original model of X. If original model is rotationally ambiguous, then factors usually change: $G[X Z]$ is different from $G(X)$ and similarly $F[Xz]$ is different from $F(X)$. These new factors fit X as well as the original factors, thus they are as quantitative as the original factors. The rotation of these new factors takes into account information from matrix Z. In some cases, the new factors are rotationally unique, without any ambiguity. More often, the ambiguity of new factors is less than the original ambiguity.

RESPONSE: This fullsome explanation is very valuable, and aspects of this background relevant to our paper have been added to the manuscript.

Discussion of the manuscript

This manuscript suffers badly from almost complete avoidance of equations and mathematical symbols and mathematical notation in general. Also, there are serious problems in the few equations that are present. A more compact and easier to read presentation is obtained if mathematical notation is used as the primary means of communication. It is possible that part of my criticism in this review is simply based on misunderstanding unclear and/or ambiguous verbal explanations of mathematical concepts.

RESPONSE: We have addressed this by a new, more mathematical description of our methods.

The ideal of scientific work is repeatability. This ms does not provide facts that might enable repeatability, even in principle. E.g., I could not find dimensions of data matrices or obtained Q values.

RESPONSE: Dimensions have been added.

How were NSD data preprocessed before PMF computations? Using averages or medians? How were outliers handled? How many factors were used in each case? And so on.

RESPONSE: This information has been added together with a reference to a report provided by the data provider, NPL.

The basic assumption of factor analytic modeling is that for each source, chemical profile and size distribution stay constant throughout the measurement campaign. On the other hand, it is well known that whenever nucleation happens, aerosol size distributions do vary. Also, largest particles tend to settle down more during longer transit times. In this work, constancy of size distributions was silently assumed. It might be good to discuss this fundamental question in future versions of this work.

RESPONSE: Point taken. This is something that we have mentioned in previous papers with reference to the assumption that the profile of the sources does not change between emission and arrival at the receptor site.

Two-stage PMF model vs. customary PMF model In the present ms, the goal was to determine the size distributions corresponding to the previously determined aerosol composition sources. It was assumed (on what grounds?) that the rotation of the original PMF result was correct, so that the originally obtained G matrix was deemed suitable for the PMF model of NSD matrix Z.

RESPONSE: We clarify the assumption that we were satisfied with the solution from the first analysis referring the reader to Beddows et al. (2015). This solution gave the best solution/rotation (agreed with all the authors during the work) to describe the urban atmosphere measured at the NK site. There are details in Beddows et al. (2015) justifying this.

In other words, it was desired that X "drive" the modeling of [X Z]. Essentially, this method corresponded to Case B, discussed above. Apparently, the authors were unaware of the one-stage method suggested for Case B.

RESPONSE: We were aware of this method but avoided it in view of having a united G factor which would not be possible with a joint matrix [X Z].

In hindsight, the best approach might have been to follow both Case B and Case C, especially if there was no positive information confirming that the original PMF model of X was rotationally unique and correct. An enhanced version of the ms should briefly discuss the one-stage possibilities of doing this work according to Case B and/or Case C.

RESPONSE: We have added two sections which describe Case B and case C.

The one-stage method, with suitably weighted X and Z, would be easier to explain and much easier to understand. However, it is not reasonable to expect that the work be redone using the one-stage approach. I understand step 2 so that the computed G factors from step 2 were forced to be practically identical to G factors from step 1. Is this right?

RESPONSE: Yes, this is correct.

If this is right, then step 2 appears to be equivalent to non-negative weighted regression (non-negative weighted linear least squares fit) of matrix Z by columns of matrix G. This should be mentioned.

RESPONSE: We have now mentioned this.

There are easy-to-use computer programs for computing such LS fits. Although PMF may also be used for this fit, using simpler tools would make the process more transparent, so avoiding unnecessary complications. Equations for defining the hidden factor should be given. The verbal definition is hard to understand and I did not manage to understand it.

RESPONSE: We hope that the clarification of the description and mathematics will mean that this is now expressed clearly.

The hidden factor, aka Nucleation factor

It is a good idea to assume that due to its higher time resolution, the NSD matrix Z may contain factors that are not visible in matrix X of chemical profiles. Unfortunately, the method for defining the hidden factor(s) in Z is questionable. First of all, why did you assume that there is only one hidden factor?

RESPONSE: The hidden factor was revealed as the intercept in the regression of the NSD values against the G1...G6 timeseries, after which, we then looked for it in the PMF analysis.

Furthermore, from the results of Beddows et al. (2015) (for which optimum solutions were derived without factor splitting), we did not anticipate another factor to be present above 7 factors (see the Venn diagram shown in Figure 1) and this constrained our search to 7 factors, i.e. we had accounted for all of the factors in Beddows et al. (2015) and saw no need to go higher.

It seems that in stage 2, 6 factors were used. This is not defined (why not) but this is how I understand the ms. Why did you not use in 2nd stage PMF a 7th (and maybe an 8th) factor that may only fit the NSD part of the data matrix? This simple arrangement would determine hidden factor(s) avoiding the bias that non-negativity constraints may introduce in your method (see below). This alternative must be mentioned in a future version of the paper.

RESPONSE: We have clarified this. We initially used 6 and then 7 to find the nucleation factor and only went to 7 factors because of the response given to the previous point, i.e. we only looked for those factors in Beddows et al. (2015).

The second Equation (3) is incorrectly formulated. Symbol j is used as a summation index on the right side. Then it cannot appear on the left side. There is a symbol "x". It is not defined, what does it mean? The text says: "The Cran R package NonLinear Minimization (nlm) (R Core Team, 2018) was used to minimise equation 3." You must not say "minimize equation". You must specify the expression that is minimized, and also specify the free variable(s) that are varied in order to minimize. I cannot understand the expression to minimize nor the free variables. For this reason, I cannot comment more on determining the hidden factor. Maybe it is properly determined, maybe not. This part of the work is certainly not reproducible by others.

RESPONSE: This equation has been correctly formulated and numbered.

Bias: It seems that the second Equation (3) is not applied to all data because of nonnegativity constraints (however, there seems to be an error in the constraints, it is impossible to guess what was really intended). When some data are excluded, this creates a bias. It is impossible to know from the outside if this bias was negligible or if it distorted the results. The bias question must be documented.

RESPONSE: No data has been excluded. All data was fitted with non-negative constraints.

Miscellaneous

Lines 415-417 in Conclusion: "This generates confidence that the NSD and PM10 factors ascribed to one source are in fact attributable to that same source." This is a very important statement, good! There are two equations numbered (3). This caused a LOT of trouble when trying to understand the discussion of the "hidden profile" a.k.a. "nucleation profile". The first Equation 3 does not appear correctly on my computer. Possibly, it uses a symbol font that is not present on my computer so that one symbol is not visible. There is also another problem in this equation: symbol "a" is used as summation index, and symbol "a" appears also on left side. A summation index cannot be present on left side. Please check your equations before

submitting new versions of the ms. Make sure that the .pdf file contains all non-standard fonts that are used e.g. in equations.

RESPONSE: Changes made to clarify this matter.

The presentation should be helpful for the reader. The symbols used in text and in equations should be defined. Example: in first Eq. (3), there is symbol j . What does it mean? Is it the index of size bin? Why not help the reader and say so? In second Eq. (3), there is again a symbol j . What is it now? Please update the ms so that symbols are used in a systematic way, in order to help the reader. The following method is recommended in order to avoid confusion with symbols:

RESPONSE: Changes made to provide clarity.

For your own use, create a table where each symbol, however trivial, is entered. When needing more symbols, check first with the table if the symbol is already reserved for another use. When you are ready, include short definitions from the table into the ms, either in a table of notation or to the location of first use of each symbol. Use customary matrix element notation whenever possible. In this way, you could avoid using scalar "a" first as an index and then vector a_j as a vector of unknowns.

RESPONSE: This system has been adopted in the interests of clarity.

Description of the linear regression model (section 2.4) is strange. I have never seen that the coefficients are called "gradients". Also, correlations should not be mentioned when discussing linear least squares. It would be best to simply show the equation. I recommend that explanation of regression be omitted, except that the equation, using matrix element notation, should be shown.

RESPONSE: Changes made as recommended.

Figure 6 is unclear. What is illustrated by the bivariate plots? Figure caption only tells that they are bivariate plots, plotted using the Openair program. Instead of naming the plotting program, it would be more important to define what is plotted vs. what, and what are the dimensions in individual diagrams. After working with the ms for a long time, I tend to guess that the "bivariate plots" might represent NSD concentrations in polar plots of wind direction and wind speed. Why did you not say this? Saving one sentence from the ms may cost hours for your new readers.

RESPONSE: A description of the Bivariate plots is given as an added section and the details requested added in the figure legend.

1
2
3
4
5
6
7
8
9
10
11
12
13
14
15
16
17
18
19
20
21
22
23
24
25
26
27

**RECEPTOR MODELLING OF BOTH PARTICLE COMPOSITION
AND SIZE DISTRIBUTION FROM A BACKGROUND SITE IN
LONDON, UK – THE TWO STEP APPROACH**

David C.S. Beddows and Roy M. Harrison*†

**National Centre for Atmospheric Science
School of Geography, Earth and Environmental Sciences
University of Birmingham
Edgbaston, Birmingham B15 2TT
United Kingdom**

*To whom correspondence should be addressed.

Tele: +44 121 414 3494; Fax: +44 121 414 3708; Email: r.m.harrison@bham.ac.uk

† Also at: Department of Environmental Sciences / Center of Excellence in Environmental Studies, King Abdulaziz University, PO Box 80203, Jeddah, 21589, Saudi Arabia

28 **ABSTRACT**

29 Some air pollution datasets contain multiple variables with a range of measurement units,
30 and combined analysis by Positive Matrix Factorization (PMF) ~~is~~ can be problematic, but
31 can offer benefits from the greater information content. In this work, a novel method is
32 devised and the source apportionment of a mixed unit data set (PM₁₀ mass and Number
33 Size Distribution NSD) is achieved using a novel two-step approach to PMF. In the first step
34 the PM₁₀ data is PMF analysed using a source apportionment approach in order to provide
35 a solution which best describes the environment and conditions considered. The time series
36 G values (and errors) of the PM₁₀ solution are then taken forward into the second step where
37 they are combined with the NSD data and analysed in a second PMF analysis. This results
38 in ~~apportioned~~ NSD data associated with the apportioned PM₁₀ factors. We exemplify this
39 approach using data reported in the study of Beddows et al. (2015), producing one solution
40 which unifies the two separate solutions for PM₁₀ and NSD data datasets together. We also
41 show how regression of the NSD size bins and the G time series can be used to elaborate
42 the solution by identifying NSD factors (such as nucleation) not influencing the PM₁₀ mass.

43 **Keywords:** PM₁₀; London; PMF; source apportionment; receptor modelling

44

45 **1. INTRODUCTION**

46 It is unquestionable that worldwide, the scientific vista of air quality is expanding; whether it
47 is the increasing number of observatories or the refinement of information mined from the
48 increasing sophistication of measurements often incorporated in campaign work. The
49 number of metrics being measured has increased from simple measurements of PM mass
50 and gas concentrations, and we can now probe the composition of the PM mass and the
51 size distributions with mass spectrometers, mobility analysers and optical devices.

52
53 Studies using PMF as a tool for source apportionment of particle mass using
54 multicomponent chemical analysis data are published ~~almost daily~~frequently using datasets
55 from around the world. However, they do not always provide consistent outcomes (Pant
56 and Harrison, 2012), and one means by which source resolution and identification can be
57 improved is by inclusion of auxiliary data, such as gaseous pollutants (Thimmaiah et al.,
58 2009), particle number count (Masiol et al., 2017) or particle size distribution (Beddows et
59 al., 2015; Ogulei et al., 2006; Leoni et al., 2018).

60
61 Harrison et al. (2011), analysed NSD data (merged SMPS and APS data) with PMF using
62 auxiliary data (meteorology, gas concentration, traffic counts and speed). The study used
63 particle size distribution data collected at the Marylebone Road supersite in London in the
64 autumn of 2007 and put forward a 10 factor solution comprised of roadside and background
65 particle source factors. Sowlat et al., 2016 carried out a similar analysis on number size
66 distribution (13nm - 10µm) data combined with several auxiliary variables collected in Los
67 Angeles. These included BC, EC/OC, PM mass, gaseous pollutants, meteorological, and
68 traffic flow data. A six-factor solution was chosen comprising of: nucleation, 2 x traffic, an
69 urban background aerosol, a secondary aerosol and a soil factor. The two traffic sources
70 made~~contributed~~ up to above 60% of the total number concentrations combined. Nucleation

71 was also observed as a major factor (17%). Urban background aerosol, secondary aerosol,
72 and soil, with relative contributions of approximately 12, 2.1, and 1.1%, respectively, overall
73 accounted for approximately 15% of PM number concentrations, although, these factors
74 dominated the PM volume and mass concentrations, due mainly to their larger mode
75 diameters. Chan et al. (2011) considered extracting more source information from an
76 aerosol composition dataset by including data on other air pollutants and wind data in the
77 analysis of a small but comprehensive dataset from a 24-hourly sampling programme
78 carried out during June 2001 in an industrial area in Brisbane. They chose multiple types of
79 composition data (aerosols, VOCs and major gaseous pollutants) and wind data in source
80 apportionment of air pollutants and found it to result in better defined source factors and
81 better fit diagnostics, compared to when non-combined data were used. Likewise, Wang et
82 al. (2017) report an improvement in source profiles when coupling the PMF model with ¹⁴C
83 data to constrain the PMF run as *a priori* information.

84
85 However, while combining, for example, particle chemical composition and size distribution
86 data in a single PMF analysis may assist source resolution, ~~it does not allow~~ difficulties arise
87 if the two datasets have different and/or ambiguous rotations (discussed in sSection 2). This
88 tends to result in factors with either mass contributions and small number contributions or
89 number contributions and small mass contributions and rarely a meaningful contribution
90 from both data types. ~~quantitative attribution of either particle mass or particle number to the~~
91 ~~source factors.~~ Experimental design can of course circumnavigate this problem, for
92 instance, using chemical data which is already size segregated, measured using a cascade
93 impactor (Contini et al., 2014). Such an approach is attractive by view of the fact that there
94 is no question as to whether both data-sets sufficiently overlap across the size bins.
95 However, ~~impact-cascaders~~ ~~impactors do not~~ ~~don't necessarily enjoy~~ offer the high time

96 resolution of particle counting instruments, with individual measurements lasting hours or
97 days. Even so, for the case where two or more instruments are available in a campaign to
98 measure two or more different metrics, e.g. PM mass and particle number and (PN), then
99 thea prescribed methodcombined data analysis is useful. Furthermore, Emami and Hopke
100 (2017) haves showned that the effect of adding variables as auxiliary data (with potentially
101 different units) to a NSD data set is to decrease the rotational ambiguity of a solution from a
102 1-step PMF analysis.

103
104 ~~Comero et al. (2009) alluded to the problem of including more than one metric with different~~
105 ~~units when citing Hopke (1991). In order to obtain a physically realistic PMF solution some~~
106 ~~natural constraints must be satisfied, one being, “Only for chemical elements or compounds,~~
107 ~~where the unit of measurement are the same, the sum of the predicted elemental mass~~
108 ~~contributions for each source must be less than or equal to total measured mass for each~~
109 ~~element; the whole is greater than or equal to the sum of its parts (only in the case of~~
110 ~~chemical elements or compounds)”.~~ This underlies the necessity to have a consistency of
111 units throughout the input dataset in order to make a quantified apportionment. To exemplify
112 this point, in

113
114 ~~The potential for an improved factor solution obtained by mixing data types in PMF provides~~
115 ~~a motivation in the community to develop a methodology which can overcome the~~
116 ~~aforementioned difficulties.~~ In this study, we present such a method for analysing
117 simultaneously collected PM₁₀ composition and NSD data. In the work of Beddows et al.
118 (2015), both particle composition and number size distribution (NSD) data from a
119 background site in London (2011 and 2012) was analysed using Positive Matrix
120 Factorization. As part of the methodology development, it was concluded that it was

121 preferable not to combine these two data types in ~~the a single~~ analysis but to conduct
122 separate PMF analyses for PM₁₀ mass and particle number. This yielded a 6 factor solution
123 for the PM₁₀ data (Diffuse Urban; Marine; Secondary; Non-Exhaust Traffic/Crustal
124 (NET/Crustal)); Fuel Oil; and Traffic. Factors described as Diffuse Urban; Secondary; and
125 Traffic were identified in the 4 factor solution for the NSD data, ~~together with a~~. ~~A further~~
126 ~~factor was the~~ Nucleation factor not seen in the PM₁₀ mass data analysis (see Figure 1).
127 When combining the PM₁₀ and NSD data in a single PMF analysis, Diffuse Urban;
128 Nucleation; Secondary; Aged Marine and Traffic Factors were identified but the factors were
129 not as clearly separated from each other as the factors derived from the separate datasets.
130 For example, Fuel Oil was now mixed in with Marine and called Aged Marine. This is
131 summarized in Figure 1. However ~~in the analysis~~, it would still be useful to obtain a number
132 size distribution for each of the 6 PM₁₀ factors and/or a chemical composition for the 4 NSD
133 factors. As a continuation of this work, we present an alternative method ~~of~~ for analysing
134 the combined dataset in a so called, two-step methodology. In the first step, we analyse the
135 mass data (PM₁₀; units: $\mu\text{g}/\text{m}^3$) according to the methodology of Beddows et al. (2015). This
136 results in a time series factor G which is carried forward into a second PMF analysis of a
137 combined data-set consisting of the G time series and an auxillary data set (~~egi.e.~~ NSD;
138 units: $1/\text{cm}^3$). The first step identifies sources and apportions the G factors to their
139 contribution to mass and in the second step, an FKEY matrix is chosen such that G 'drives'
140 the model and the NSD data 'follow'. This means that we have PM₁₀ factors each of which
141 ~~are is~~ augmented by its number size distribution. Furthermore, we also consider linear
142 regression as a second step in a PMF-LR analysis to show that although the initial analysis
143 is biased toward mass by analysing PM₁₀ factors only, seen-unseen factors influencing the
144 NSD data (e.g. nucleation) can be identified in the data.

145

146 2. EXPERIMENTAL

147 With a population of 8.5 million in 2014 (ONS, 2017), the UK city of London is the focus of
148 study in this work where the London *North Kensington* (NK) Site ($LAT = 51^{\circ} : 31' : 15.780''$
149 N and $LONG = 0^{\circ} : 12' : 48.571''$ W) was considered. NK is part of both the London Air
150 Quality Network and the national Automatic Urban and Rural Network and is owned and
151 part-funded by the Royal Borough of Kensington and Chelsea. The facility is located within
152 a self contained cabin within the grounds of Sion Manning School. The nearest road, St.
153 Charles Square, is a quiet residential street approximately 5 metres from the monitoring site
154 and the surrounding area is mainly residential. The nearest heavily trafficked roads are the
155 B450 (~100 m East) and the very busy A40 (~400 m South). For a detailed overview of the
156 air pollution climate at North Kensington, the reader is referred to Bigi and Harrison (2010).

157

158 2.1 Data

159 ~~For this study~~As alluded to, this work is a continuation of the study carried out by Beddows
160 et al (2015), which analysed ~~chemical~~ NSD and PM₁₀ ~~chemical composition~~ data ~~were~~
161 collected at the London NK receptor site. ~~the same datasets considered, and PMF analysis~~
162 outputs generated, by Beddows et al. (2015) were used. For this, 24h air samples were
163 taken daily over a two year period (2011 and 2012) using a Thermo Partisol 2025 sampler
164 fitted with a PM₁₀ size selective inlet, and alongside, Number Size Distribution (NSD) data
165 were collected continuously every ~~¼ hour~~ 15 min using a Scanning Mobility Particle Sizer
166 (SMPS) consisting of a CPC (TSI model 3775) combined with an electrostatic classifier (TSI
167 model 3080) ~~and~~ air dried according to the EUSAAR protocol (Wiedensohler et al., 2012).
168 The particle sizes covered were 51 size bins ranging from 16.55 nm to 604.3 nm ~~and the 15~~
169 min distributions were aggregated up to hourly ~~samples~~ averages (where there were at least
170 3 x 15 min samples per hour) and all missing values were replaced using a value calculated

171 using the method of Polissar et al. (1998). Further details of the SMPS settings are given in
172 Table S1 and. ~~Analysis of this data resulted in PMF source profiles F and source time series~~
173 ~~G of the PM₁₀ and NSD data sets which were carried forward into this work.~~ Further details
174 of the data, collection methods, coverage and first analysis are given in Beddows et al.
175 (2015)—the reader is also referred to Becceaceci et al. (2013–a,b) for an extensive
176 ~~study~~account of how the NSD data was collected and quality assured.

177
178 Accompanying the NSD data from the study of Beddows et al. (2015) was the PMF output
179 from the analysis of ~~Analysis of this data resulted in PMF source profiles F and source time~~
180 ~~series G of the PM₁₀ chemical PM₄₀ composition data. PM₁₀ and NSD data sets which were~~
181 ~~carried forward into this work.~~ The latter data consisted of 24h air samples taken daily over
182 a 2-year period (2011 and 2012) using a Thermo Partisol 2025 sampler fitted with a PM₁₀
183 size selective inlet. These filters were analysed for total metals PM_{metals} (Al, Ba, Ca, Cd, Cr,
184 Cu, Fe, K, Mg, Mo, Na, Ni, Pb, Sn, Sb, Sr, V, and Zn), using a Perkin Elmer/Sciex ELAN
185 6100DRC following HF acid digestion of GN-4 Metrical membrane filters. ~~Similarly, w~~Water-
186 soluble ions PM_{ions} (Ca²⁺, Mg²⁺, K, NH₄⁺, Cl⁻, NO₃⁻ and SO₄²⁻) were measured using a
187 near-real-time URG-9000B (hereafter URG) ambient ion monitor (URG Corp). The data
188 capture over the 2 years ranged from 48 to 100% as different sampling instruments varied
189 in reliability. ~~These Data~~ gaps were filled by measurements made on daily PM₁₀ filter
190 samples collected continuously at this site using a Partisol 2025; laboratory-based ion
191 chromatography measurements were made for anions on Tissuquartz™2500 QAT-UP
192 filters). No cation measurements were available from these filters, and this resulted in ~~thea~~
193 lower data capture for the cations. ~~But a~~Again, all missing data were replaced using a value
194 calculated using the method of Polissar et al. (1998). A woodsmoke metric, CWOD, was
195 also included. This was derived as PM Woodsmoke from the methodology of Sandradewi

196 et al. (2008) utilising Aethalometer and EC/OC data, as described in Fuller et al. (2014).
197 Samples were also collected using a Partisol 2025 with a PM₁₀ size selective inlet and
198 concentrations of elemental carbon (EC) and organic carbon (OC) were measured by
199 collection on quartz filters (Tissuquartz™ 2500 QAT-UP) and analysis using a Sunset
200 Laboratory thermal–optical analyser according to the QUARTZ protocol (which gives results
201 very similar to EUSAAR 2: Cavalli et al., 2010) (NPL, 2013). We refer to CWOD, EC and
202 OC as PM_{carbon}. In addition, particle mass was determined on samples collected on Teflon-
203 coated glass fibre filters (TX40HI20WW) with a Partisol sampler and PM₁₀ size-selective
204 inlet.

205
206 This aforementioned PM₁₀ data was represented in this work as the PMF solution for PM₁₀-
207 only data, derived in Beddows et al. (2015) and consisting of 6 sources, namely: Diffuse
208 Urban; Marine; Secondary; Non-Exhaust; Traffic/Crustal; Fuel Oil; and Traffic. The Diffuse
209 Urban factor had a chemical profile indicative of contributions mainly from both woodsmoke
210 (CWOD) and road traffic (Ba, Cu, Fe, Zn). The Marine factor explained much of the variation
211 in the data for Na, Cl⁻ and Mg²⁺, and the sSecondary factor was identified from a strong
212 association with NH₄⁺, NO₃⁻, SO₄²⁻ and organic carbon. For the tTraffic emissions, the PM
213 did not simply reflect tailpipe emissions, as it also included contributions from non-exhaust
214 sources, i.e. resuspension of road dust and primary PM emissions from brake, clutch and
215 tyre wear. The nNon-eExhaust tTraffic/eCrustal factor explained a high proportion of the
216 variation in the Al, Ca²⁺ and Ti measurements consistent with particles derived from crustal
217 material, derived either from wind-blown or vehicle-induced resuspension. There was also
218 a significant explanation of the variation in elements such as Zn, Pb, Mn, Fe, Cu and Ba,
219 which had a strong association with non-exhaust traffic emissions. As there was a strong
220 contribution of crustal material to particles resuspended from traffic this likely reflected the

221 presence of particulate matter from resuspension and traffic-polluted soils. The last factor
222 was attributed to fFuel eOil, characterised by a strong association with V and Ni together
223 with significant SO₄²⁻. This output comprised the first-step solution in the 2-step analysis of
224 PM₁₀ and NSD data and in this study we concentrate on the analysis of the NSD data in the
225 second PMF step with the aim of assigning a NSD to each of the 6 PM₁₀ factors.

226

227 **2.2 Proxy Data**

228 As alluded to in the introduction, experimental design can ensure that measurements cover
229 the the same particle size range by using a single instrument such as a cascade impactor
230 which gives size and mass information. However for our case, the NSD spanned anthe
231 aerodynamic particle sizes 0.10 — 0.88 μm (i.e. PN_{0.9}) which is smaller than the range
232 covered by the particulate mass, ≤10 μm, i.e. PM₁₀.

233

234

235 Besides the The value of PM₁₀ is given by the measured PM₁₀ mass, and tThe PM_{0.9} mass
236 is calculated by equation 3 1 from the NSD assuming estimates of PM mass can be derived
237 using the NSD assuming spherical particles of a fixed density. For the SMPS settings, a
238 particle size range between 16 and 604 nm is collected which can beand was used to
239 estimate a PM_{0.96} value using equation 1.

$$PM_{0.96} = \rho_{eff} \times \frac{\pi}{6} \sum_{sizeBins} d^3 \quad (3 \quad 1)$$

240

241 Where ρ_{eff} is set to 2 g/cm³ (for the whole time series and across all size bins) for a Diffuse
242 Urban background (based taken as the rounded midpoint of the rangeupon 1.8-2.5 g/cm³

243 for an urban background aerosol; Beddows et al., 2010). Due to the approximations used
244 in this proxy variable, a large uncertainty was applied to it in the PMF analysis so not to
245 affect the result.

246

247 Figure S1 plots the total apportioned PM_{10} mass against the $PM_{0.96}$ estimates and shows
248 that although the SMPS does not account for the whole mass, it does track with the total
249 PM, with a fitted gradient of 0.635, i.e. accounting for 635% of the mass. To account for the
250 particles greater than 600 nm in the PMF analysis, a proxy was used created by using the
251 difference between the total daily apportioned PM mass in the step 1 of the PMF analysis
252 and the mass estimated from the SMPS data. This difference was then converted back into
253 a number and added to the NSD matrix of counts as $PN_{0.6-10}$ to improve the match of the
254 NSD matrix to the PM_{10} . This was appended as a column in to the input matrix of the PMF
255 analysis with uncertainties taken as the $4 \times PN_{1.0-10}$, so not overly influence the analysis.

256 With the consideration of future measurements where this method was to be applied, an
257 improved result might be possible if $PM_{1.0}$ was used in preference to PM_{10} in order to give a
258 better match between the size ranges of the mass and number data, if only, to close any
259 uncertainty over the the issue. Another alternative is simply to include an APS in the
260 measurements and merge the APS data to the SMPS data as in Beddows et al. (2010).
261 This would provide a complete overlap between the NSD and PM_{10} data.

262

263 **2.3.2** Methods

264 **2.3.2.1** PMF

265 Positive Matrix Factorization (PMF) is a well-established multivariate data analysis method
266 used in the field of aerosol science. PMF can be described as a least-squares formulation

267 of factor analysis developed by Paatero (Paatero and Tapper, 1994). It assumes that the
 268 ambient aerosol concentration X (represented by $n \times m$ matrix of n observations and m PM₁₀
 269 constituents or NSD size bins), measured at one or more sites, can be explained by the
 270 product of a source profile matrix F and source contribution matrix G whose elements are
 271 given by equation 41:

$$x_{ij} = \sum_{k=1}^p g_{ik} \cdot f_{kj} + e_{ij} \quad i=1 \dots n; j=1 \dots m \quad (41)$$

272 where the j^{th} PM constituent (element, size bin, or auxiliary measurement) on the i^{th}
 273 observation (i.e. hour) is represented by x_{ij} . The term g_{ik} is the contribution of the k^{th} factor
 274 to the receptor on the i^{th} hour, f_{kj} is the fraction of the j^{th} PM constituent in the k^{th} factor, and
 275 e_{ij} is the residual for the j^{th} measurement on the i^{th} hour. The residuals (i.e. difference
 276 between measured and reconstructed concentrations) are accounted for in matrix E and the
 277 two matrices G and F are obtained by an iterative algorithm which minimises the object
 278 function Q (see equation 52).

279
 280 ~~Given,~~ Using the data and uncertainty ~~to~~ matrices for the model, equation 41 is optimised in
 281 the PMF2 algorithm by minimising the Q value (equation 22),

$$Q = \sum_{i=1}^n \sum_{j=1}^m \left(\frac{e_{ij}}{s_{ij}} \right)^2 \quad (52)$$

282
 283 where s_{ij} is the uncertainty in the j^{th} measurement for hour i . All analyses were carried out
 284 in Robust model which reduces the impact of outliers (Paatero, 2002).

285

286 ~~It may be seen from equation (2) that~~ PMF is a weighted technique; ~~and~~ the value of Q,
287 and hence the model fit, is determined by the input variables with the lowest values of
288 uncertainty, ~~S_{ij}~~ , ~~thus giving their variables a higher weighting in the analysis~~. Input
289 variables with ~~low weight high uncertainty~~ have little effect upon the value of Q, even when
290 their residuals are large. This can be used to the advantage of the operator, ~~e.g. when~~.
291 ~~When~~ apportioning total PM mass in a conventional one-~~stepstage~~ PMF, the total PM
292 concentrations are normally input with artificially high uncertainty, so that they are essentially
293 passive in the PMF analysis and do not influence its outcome. By doing so, the chemical
294 composition data determine the apportionment of PM mass to the source-related factors
295 identified by the PMF. ~~A similar approach can be followed in the PMF analysis of a combined~~
296 ~~data-set where higher weightings can be applied to the main data-set of interest such that it~~
297 ~~“drives” the analysis and the auxillary data set “follows”, i.e. the uncertainties are chosen~~
298 ~~such that the balance of total weights from the two data sets is tipped towards the~~
299 ~~measurement of interest and highest reliability in regards to of rotational unambiguity. In this~~
300 ~~work, the primary aim was to define a particle size distribution associated with each factor~~
301 ~~derived from the PMF of PM₁₀ composition. Consequently, in the second stage of the PMF,~~
302 ~~large uncertainties were input for the particle number data, combined with realistic~~
303 ~~uncertainties for the PM G-values, so that the latter determine the outcome of (“drive”) the~~
304 ~~PMF analysis.~~

305

306 ~~To assess the PMF model, the~~ In this work, the Q value is outputted by PMF2 and
307 compared to a theoretical value Q_{theory} which is approximately the difference between the
308 product of the dimensions of X and the product of the number of factors and the sum of
309 dimensions of X (i.e. $n \times m - p(n + m)$) $p \times m$. For a given number of factors, the whole
310 uncertainty matrix is scaled by a factor ~~X_{scale}~~ b_{scale} until the ratio between Q and Q_{theory} is

311 approximately one (rQ value = $Q/Q_{\text{theory}} \approx 1 \pm 0.02$).

312

313 With regards to the final output from PMF, a scaling has to be applied in order to achieve
314 quantitative results. This is done by scaling either G or F to unity such that the units from
315 X are carried over to either F or G respectively to complete the apportionment. However,
316 different routes have to be considered depending on whether X has homogeneous or
317 heterogeneous units.

318

319 2.32.2 1-Step method using data from the same instrument in the same units -

320 Hhomogeneous units

321 Given a PMF input data matrix X, a solution $GF + E$ can be computed where G represents
322 the time series of the source profiles F, with a residual matrix E. Often X comprises of
323 columns of PM₁₀ composition values component concentrations (e.g. ICPMS values
324 measured from quartz filters acid-digested filters collected with a Partisol 2025) and it is
325 common practice to also include a Total Vvariable (e.g. column of PM₁₀, measured using a
326 TEOM) in the data matrix. The resulting PM₁₀ profile element value can then be used to
327 scale G and F such that G carries the units of X with F unit-less. Note that neither G or F is
328 scaled to unity in this approach. Instead, scaling is done after the analysis using a constant
329 a_k , determined by the time series of a Total Vvariable (e.g. PM₁₀), down weighted by a factor
330 of 4 applying a high uncertainty, within the input data.

331

$$x_{ij} = \sum_{k=1}^p (a_k g_{ik}) \left(\frac{f_{kj}}{a_{zk}} \right) \quad (63)$$

332

333 The resulting value for the PM₁₀ contribution for each factor within the F matrix is then used
334 as a scaling constant a_k in equation 63. Such scaling results in unit-less factors F which
335 describe the characteristics of the sources and time series G with units of $\mu\text{g}/\text{m}^3$.
336 Apportionment can then be carried out by averaging the G values for each source
337 ~~profile factor, and/or~~ a fully quantified time series of each factor can be presented, e.g. in
338 Bivariate plots. Of course, the G and F can be normalized such that G is unitless and F
339 carries ~~the~~ units; an approach necessary when X ~~contains~~ heterogeneous units.
340 This approach however, requires ~~each column of G~~ to be scaled to unity, by using the PMF
341 setting Mean IGI = 1.

342
343 2.32.3 1-Step method using data ~~from different instruments with different units~~ -
344 ~~H~~heterogeneous units

345 If the analysis of X was to be enhanced by the inclusion of data from a second instrument
346 with different units, then a different approach to the 1-Step method with ~~H~~homogeneous
347 units would be required to analyse the joint data matrix $[X,Z] = G[X,Z] F[X,Z] + E[X,Z]$. If the
348 previous method was applied where F was normalized, then it would not be clear what units
349 to assign to G, whether the units from X or Z. To get around this problem, G is scaled to
350 unity. This results in a unit-less time series G and a quantified F matrix. For each source
351 profile the sum of the species associated with either data type gives the average total
352 apportionment, e.g. of PM₁₀ or number concentration PN. Of course, this requires the
353 complete mass or number closure of the elements making up either PM₁₀ or PN respectively,
354 although inclusion of measurements of total PM₁₀ or PN can used instead, if available.

355
356 In the ideal case, if the individually computed factors for both data sets result in G(X) and
357 G(Z) being identical, then a straight-forward joint model $[X,Z]$ is successful and $G[X,Z] =$

358 G(X) = G(Z). However, if G(X) and G(Z) are significantly different then the joint model will
359 fail, identified by a too large Q value. A solution to this problem is to set the total weights of
360 the better dataset X significantly higher than the total weights of the auxiliary data set Z such
361 that X will “drive the model” and G[X,Z] will be approximately equal to G(X) and a reasonable
362 Q value is obtained for the Z. However, care is required to ensure that X or Z do not contain
363 rotational ambiguity because such rotation for X may not be suitable for Z. For such cases,
364 equal total weights for both X and Z are applied in the hope that the best rotation for both X
365 and Z can be found.

366

367 2.32.4 2-Step method using data ~~from different instruments with different units~~ -
368 ~~H~~heterogeneous units

369 The method proposed in this work, separates the analysis of the two data sets X and Z into
370 two different PMF analyses. Dataset X is first analysed and an unambiguous rotation is
371 selected which gives computed factors G(X). These are then carried over into a second
372 PMF step in which G(X) are combined with Z to form a joint matrix for analysis. By using
373 FKEY (described below) factors, G(X,Z) are forced to be equal to G(X) from step 1. So for
374 example, if in the first step we analyse PM₁₀ data and carry forward the output G(PM₁₀) into
375 a second step combined with the NSD data, i.e. [G(PM₁₀),NSD] this results in profiles
376 F[G(PM₁₀),NSD]. In other words, we force out of the NSD data source profiles which have
377 the same G factors as the PM₁₀ data and extend the list of components of the sources
378 identified in the first step and thus improve ~~identification~~ characterisation of the source.
379 Note that this is equivalent to non-negative weighted regression of matrix Z by columns of
380 matrix G for which ~~other~~ tools exist. Furthermore, by using a two step method, we can
381 continue to use the scaling method described in Section 2.32.2 to apportion the sources
382 using a quantified time series G(X) rather than normalising the G(X,Z) matrix sums to 1 and

383 relying on the summation of the elements in the rows of F(X,Z) to give the apportionment of
384 X and Z.

385

386 **2.3.22.5. Application of PMF**

387 Positive Matrix Factorization was carried out in this work using the DOS based executable
388 file PMF2 v4.2 compiled by Pentti Paatero and released in Feb 11, 2010 (downloaded
389 from www.helsinki.fi/~paatero/PMF/). This is used by the author ~~as a~~ preference to a GUI
390 version of PMF (e.g. US EPA PMF 5.0, Norris et al., 2014)) because of the ease with which it
391 can be ~~encompassed~~ incorporated into an R procedure script using shell commands,
392 thus facilitating automation of the analysis and any optimisation. R-script can be written to
393 manipulate and organise input data for PMF2, run PMF2, collect the output and produce the
394 necessary output for consideration as text, table or plot. The main strength for this approach
395 is to improve the repeatability and transferability of a method between practitioners within
396 our group.

397

398 The two step method is shown schematically in Figure 2. Matrix X yields factors 1G and 1F
399 in the first step. The timeseries 1G matrix is carried through to the second step where it is
400 combined with an auxiliary data set Z, to give the a step 2 input matrix [1G Z]. This in
401 turn is analysed to produce factors 2G and 2F . In the current example, it uses the PMF
402 output of the dataset of Beddows et al. (2015) is used as a starting point matrix X and
403 comprises assumes that a PMF analysis of the PM₁₀ chemical composition dataset. This
404 yields timeseries 1G and source profile 1F and the reader is referred to Beddows et al. (2015)
405 for a description of the analysis and output. Figure 1 shows the output from the first step
406 which was found to be the optimum solution after considering 3 to 8 factor solutions.

407 ~~(Step One) has already been carried out and dealt with as in the previous study. The~~
408 ~~normalised timeseries matrix 1G from this analysis ~~were~~was combined with the NSD data -~~
409 ~~concurrently measured with the PM_{10} data - to form the input matrix [1GZ], for step 2. In this~~
410 ~~current work, a second step which takes the output from the first step and uses it as an input~~
411 ~~for the second step is developed. This is done by using the G1 time series from the PMF~~
412 ~~analysis of PM_{10} and combining this with secondary data, (i.e. NSD data). The uncertainties~~
413 ~~of the 1G1 matrix, ${}^1\Delta G$ are transferred from the output of the first step and entered as input~~
414 ~~uncertainties for the second step. The hourly NSD data was aggregated into daily~~
415 ~~samples values to match the daily 1G factors outputted from the PMF analysis of the daily~~
416 ~~PM_{10} data sampled. This reduced the data matrix down to 590 rows by ~~57~~ ~~52~~ columns~~
417 ~~(${}^1G1...{}^1G6, NSD_1^{16nm}...NSD_{51}^{640nm}$) for which we have a Q_{theory} value of ~~29748~~ ~~30,916~~ for~~
418 ~~a 6 factor solution. For the NSD data, the uncertainties are taken as ~~X~~ times the NSD values~~
419 ~~multiplied by the value of an arbitrary parameter b_{scale} in order to be large and ensure that~~
420 ~~the PMF is driven by the G1 matrix (see Figure 2). Initially, ~~this~~ b_{scale} was set to 4 to ~~in order to~~~~
421 ~~ensure that the model was weighted such that it was driven by the PM_{10} data. However, this~~
422 ~~operation becomes somewhat redundant by the use of the FKEY matrix discussed in the~~
423 ~~next section. However, in order to find the optimal NSD uncertainties ~~the~~ The value of ~~X~~ ~~the~~~~
424 ~~parameter b_{scale} (typically, 0.2) was optimised in Cran R so that the ratio of $Q/Q_{theory} = 1 \pm$~~
425 ~~$0.042 \sim 1$, indicating an relative percentage uncertainty in the region of 20%. In retrospect -~~
426 ~~by taking into account the decrease in reliability of the size bins counts towards the edges~~
427 ~~of the size bin range - an improvement would be to gradually increase the uncertainties from~~
428 ~~5-% in the middle range of sizes over the lower and upper size bins from 5-% ~~upto~~ to a pre~~
429 ~~defined larger value, e.g. 50-%, over the lower and upper size bins. The uncertainties were~~
430 ~~entered directly into the model using PMF matrix T with U and V redundant.~~

431

432 Using equation 7 the uncertainties were entered directly into the model using via matrix T
433 with U and V redundant.

$$s_{ij} = t_{ij} + u_{ij} \sqrt{|x_{ij}|} + v_{ij} |x_{ij}| \quad (7)$$

434

435 **2.3.32.6 Fkey Pulling down with GKEY and FKEY**

436 GKEY and FKEY key are is a feature matrices with the same dimensions of as G and F
437 respectively, in for incorporating a priori information into a PMF analysis. They are and is
438 used in the second step of the PMF-PMF analysis. It is used to “pull” elements of the source
439 profiles to zero. This method uses a matrix that GKEY and FKEY indicates the location of
440 suspected zeros in source profiles ²F or contributions ²G (Figure S123). Since here it is we
441 are concerned with the profiles, this information is given in the form of integer values in an
442 FKEY key. The greater the certainty that an element of a source profile is zero, the larger the
443 integer value that is specified. In this case, in the second step, for the input dataset [¹G
444 NSD], it is certain that only one unique contribution will be strong for each row of the profile
445 ²F, outputted from the second PMF analysis, PM G score from one of the sources will be
446 strong, e.g. only ¹G1 and not ¹G2.. ¹G6 will contribute the to (¹G1, ²F₁) position in output
447 factor ²F₁. e.g. the traffic source will be the only contributing to the PM G value in the Traffic
448 NSD profile, and likewise for the other sources: Diffuse Urban; Secondary; Marine; Fuel Oil;
449 and NET & Crustal (Figure S123). All ‘non-zero’ elements within the output of ²F take a
450 FKEY value of zero whereas all elements of ²F which are pulled to zero take an non-zero
451 value of fkey₁. This leads to a FKEY matrix which can be understood in two parts. The first
452 part is a square matrix of dimension equal to the number of columns of ¹G with all its entries
453 equal to fkey₁ except for the leading diagonal; this part ensures that ¹G is the same as ²G.
454 The second part of the matrix consist of all the elements areas zero and represents the NSD

455 input data. An $fkey_1$ value of 7 to 9 is considered a medium to strong pull, and in this work,
456 we used a value of 24 which in comparison is very aggressive ensuring only one rotational
457 solution is available ensuring $^1G \approx ^2G$.

458
459 To extend the analysis from 6 factors to 7 factors an extra row was added to FKEY. This
460 was done in order to investigate any factors missed in the NSD data ~~for~~ which the first
461 analysis using PM_{10} would not be sensitive to. For example, a nucleation mode would be
462 detected in NSD data but not PM_{10} data. In order to give the model freedom to factorise out
463 a nucleation factor, the 7th row of of FKEY values consisted $\{fkey_1, fkey_2... fkey_6, nsd_1, nsd_2...$
464 $nsd_{51}\}$. This ensured that all the 2G contributions were allocated to the first 6 factors only
465 leaving the 7th factor to account for the remaining unfactorised NSD data. There is no reason
466 why more than 7 factors could ~~not~~ be used to investigate ~~to see if there are more possible~~
467 ~~un-resolved~~unresolved NSD factors. However, we constrained the scope of our
468 investigation to reidentifying those in Figure 12.

469

470 **2.4.3 Regression**

471 ~~The output of the regression of a dependent variable Y regressed against independent~~
472 ~~variables $X_1, X_2, X_3, \dots X_n$ is n gradients and one intercept. When $n = 1$ it yields a line,~~
473 ~~when $n = 2$ it is a fitted plane. But when $n > 2$ or in this case $n = 6$, it is a multidimensional~~
474 ~~fitted model. Each of the n gradients show how Y varies with the n X values given that the~~
475 ~~other X values are fixed and the intercept provides a bias value. If Y is allowed to take on~~
476 ~~each value of the NSD size bin and X variables are set to the 6 G time series from the first~~
477 ~~step of PMF analysis, then it can be seen how the NSD are correlated to the 6 G time series~~
478 ~~and infer an associated NSD for each of the factors derived in the first step of the PMF-LR~~
479 ~~analysis.~~

480

481 As an alternative to using PMF in the second step, a regression was carried out. Each
482 column of data for each of the 51 size bins j within the NSD was regressed against the six
483 ~~$1G_1$~~ time series using, Equation ~~834~~.

$$NSD_j = \alpha_{0,j} + \alpha_{1,j} {}^1G_1 + \alpha_{2,j} {}^1G_2 + \dots + \alpha_{6,j} {}^1G_6 \quad (\underline{84})$$

484

485 where α_0 is the population intercept and α_{1-6} are the populations slope coefficients. This
486 results in a 7 by 51 matrix of values. Each column represents a size bin of the NSD data
487 and each row represents the slope coefficients associated with 6 of the factors (giving an
488 indication of how each size bin correlates scales with each of the 6 factors) and an intercept.
489 When ~~$\alpha_{1-6,j}$~~ ~~$grad_{a,j}$~~ is plotted against the size bin, 6 plots showing the dependence of each
490 size bin j on each of the 6 PM₁₀ factors are produced. It is also assumed that these (we
491 refer to-referred to here as NSD regression source profiles) will be comparable to the actual
492 NSD PMF source profile. Similarly, the ~~$\alpha_{0,i}$~~ ~~int_j~~ values are expected to give a background
493 value due to, possibly to noise; however, it is more likely to yield a source (such nucleation)
494 to which the PM₁₀ mass analysis is insensitive. ~~However, this method can extract~~
495 ~~information known as a remainder factor, shown later in this paper.~~

496

497 **2.5.4 Peak Fitting**

498 If it is assumed that the factors derived from the daily NSD data are the same as those
499 present in the hourly data, i.e. the factors are conserved when averaging the data from
500 hourly to daily data before PMF analysis, then daily NSD profiles can be fitted to the hourly
501 NSD spectra to recover a diurnal cycle for the factors. However, it is worth noting that the

502 process of aggregating hourly data to daily NSD data may indeed cause loss of information
 503 implying that minor factors (e.g. due to event episodes) might well be averaged out of the
 504 data. Given the i^{th} number size distribution, NSD_i , the difference $D_{i,j,k}$ (equation 3), between
 505 the k^{th} element and the linear superposition of the k^{th} element of the seven factors $f_{j,k}$ is
 506 minimised. Given the j^{th} size bin in the i^{th} number size distribution $NSD_{i,j}$ (of dimensions M
 507 x N), the factors can be fitted using equation (95).

$$D_i = \sum_{i=1}^M d_i \quad (95)$$

508 which is the i^{th} sum D_i of the difference (of give by equation 6) across the size bins of the i^{th}
 509 NSD_i and the linear superposition sum of the p factors NSD source profiles ($p = 7$ in this case)
 510 scaled by with respect to the scalar values c_{ik} , representing the timeseries of each fitted NSD
 511 source profiles as shown by equation 10.

$$d_i = \sum_{j=1}^N \left\{ NSD_{ij} - \sum_{k=0}^p c_{ik} \times f_{kj} \right\}, \quad c_{ik} \geq 0 \quad (106)$$

$$1 \times 10^{10}, \quad c_{ik} < 0$$

512

513 The Cran R package Non-Linear Minimization (nlm) (R Core Team, 2018) was used to
 514 minimise equation the value of D_i with respect to the scalar values c_{ik} 3. A with a non-
 515 negative constraint is on c_{ik} placed in the function. If a negative value is returned by any of
 516 the $a_k - c_k$ values then D returns an excessively large value. Furthermore, in order to extract
 517 an apportionment to number concentration ($1/\text{cm}^3$) the fitted values were scaled using a
 518 factor scalar β_k . Six-Seven values were derived for β_k by regressing the total particle number
 519 (total hourly SMPS) against each of the fitted values c_k (using equation 119). 7-7.

$$PN = \beta_0 + \beta_1 c_1 + \beta_2 c_2 + \dots + \beta_7 c_7 \quad (117)$$

520 The resulting scaled-fitted values were then used to calculate the PN concentration for each
521 of the regression source profiles (equation-12 8) and plot allowing subsequent plotting of the
522 7 diurnal cycles in Figure 5.

$$PN_k = \beta_k c_k \quad (128)$$

523

524 **2.65 Bivariate Plot**

525 Identification of the sources responsible for the factors outputted from PMF can be assisted
526 by meteorological data. Time series of the k_{th} factor (or g_k values) can be plotted against
527 wind direction and wind speed using either the polarPlot or polarAnnulus functions provided
528 in the Openair package. Polar Plots are simply used for plotting the factor contribution on a
529 polar coordinate plot with North, East, South and West axes. Mean concentrations are
530 calculated for wind speed-direction 'bins' (e.g. 0-1, 1-2 m/s,... and 0-10, 10-20 degrees etc.)
531 and smoothed using a generalized additive model. Each bin concentration is plotted as a
532 group of pixels (coloured according to a concentration-colour scale) and positioned a
533 distance away from the origin according to the magnitude of wind speed and along an angle
534 from the North axis according to the wind direction. Such plots are useful when identifying
535 the nature of the source. A backgrounddiffuse source will tend to have its highest
536 concentration yield showing as a hotspot at the origin of the polar plot, whereas a point
537 source will cause a hotspot both away from the origin and in the direction pointing towards
538 the source. On the other hand wind blown sources tend to be recognised by their
539 proportionalityrelation to wind speed and hence do not necessarily produce hotspots.
540 Instead, they produce a minimum to maximum gradual gradient of colour from the origin,
541 spreading radially out towards the edge of the plot in the direction of the source, e.g. for a
542 marine source. Likewise, Annulus Plots, plot the mean factor concentration on a colour
543 scale by wind direction and as a function of hour-of-the-day as an annulus, represented by

544 the distance of the coloured pixels from the origin. The function is good for visualising how
545 concentrations of pollutants vary by wind direction and hour of the day. For example, for
546 the North Kensington site – positioned West of the ~~central-city centre~~ – we might well expect
547 most of the anthropogenic sources (traffic, diffuse urban, etc) to ~~haveshow~~ an Easterly
548 direction with the appropriate diurnal cycle (e.g. ~~yeilding~~ rush hour traffic patterns). Similarly,
549 we might expect cleaner air (Marine, Nucleation, etc) to occur from a Westerly direction and
550 ~~duringat times of~~ the day when the solar strength is highest.

551

552 3. RESULTS AND DISCUSSION

553 The aim of this work has been to show how, ~~given a given~~ PMF result, ~~it can be~~
554 complemented with concurrently measured auxillary data. We exemplify this using PM₁₀
555 and NSD data collected from the North Kensington receptor site in London and start with
556 the premise that we are completely satisfied with the PM₁₀ analysis and are using a rotation
557 which gives quantified factors (quantified G and scaled F) which best representation of the
558 urban atmosphere sampled, i.e. the output from Beddows et al. (2015). ~~And, f~~For each
559 PM₁₀ factor we wish to assign a NSD distribution. ~~is to take the results from the first step of~~
560 a PMF analysis where a successful source apportionment study has been completed and
561 then complement the results with a second step to derive further information about the
562 sources. ~~—~~Rather than repeat the ~~PMF~~ analysis using a combined PM₁₀+NSD
563 ~~analysisdataset~~ which can be complicated if the rotations of the individual PMF analyses of
564 PM₁₀ and NSD data are ~~miss-matched~~ or ~~ambiguous~~, we can carry out a ~~This can be done~~
565 using a second PMF analysis or a regression.

566

567 Further, by the nature of any factor analysis, we also have to make the assumption
568 that each source chemical profile and size distribution not only remain unchanged between

569 source and receptor but that it remains constant throughout the measurement campaign.
570 This of course limits our capacity to fully understand the aerosol within the atmosphere we
571 are considering. Chemical reactions during the transit of the air masses will of course modify
572 the chemical composition. ~~We might well~~ It might be assumed that a fully aged aerosol
573 remains unchanged and is identified as a background component, but for example we would
574 expect progressive chlorine depletion within a fresh marine aerosol passing over a city.
575 Likewise, we also have to appreciate that different particle sizes will ~~indeed~~ have different
576 atmospheric transit size efficiencies with large particles settling out of the air mass before
577 smaller ones. Similarly, particles nucleate and grow from 1 nm up to 20-30 nm over a short
578 time period of time. It is these finer details which are missed when making an overall
579 assessment of the chemical and physical nature composition of the air mass measured
580 over a long period (e.g. 2 years) dataset (eg 2 year)-using PMF.

581

582 **3.1 2-Step PMF-PMF Analysis**

583 Figure 3 presents ~~our results~~ the profiles 1F_k and 2F_k from the first and second PMF analysis
584 respectively of a combined dataset. The plots of 1F_k were carried over from Beddows et al.
585 (2015) to complete the assignment of the source profiles.

586

587 The ~~G1~~ time series 1G_k and uncertainties ${}^1\Delta G_k$ from the first PMF analysis of PM₁₀ data
588 we are carried over into the second step where they are combined with the NSD data for
589 PMF analysis (Figure 2). The uncertainties of the NSD data are taken as an optimised
590 multiple of the NSD values themselves (~ 5 % uncertainty, yielding a Q value of 30,333 in
591 the robust mode; see Table S2 for PMF settings). Also in order to maintain the solution from
592 step 1 in step 2 the encourage 2G_k to be proportional to 1G_k for $k = 1-6$ (see Table S4), the

593 FKEY matrix is applied to pull elements in the source matrix to zero as described in
594 section 2.3.3. This ensures that the PMF analysis of the NSD data was driven by the 1st
595 time series and. This results in a 6 factor output in which there are unique
596 contributions from the k^{th} factor 1G_k from the first analysis to the k^{th} factor from one of the
597 $G_1^2F_k$ scores and an in the second analysis. This is mainly due to the aggressive pulling
598 of the factor element in 2F applied using FKEY.

599
600 ~~associated NSD source profile, and it is~~ When inspecting Figure 3 it is notable that they the
601 source profiles are surprisingly similar to those calculated for the just-NSD and PM₁₀+NSD
602 data in Beddows et al. (2015). The Diffuse Urban factor has a modal-diameter just below
603 0.1 μm which is comparable to the NSD same factor in the just-NSD analysis. Marine is
604 comparable to the Aged Marine factor derived from the PM₁₀+NSD analysis. The Secondary
605 factor is again the factor with the largest modal diameter (between 0.4 and 0.5 μm) and
606 traffic has as expected a modal diameter between 30 and 40 nm. The Fuel Oil factor is
607 interesting as it appears to be a combination of a nucleation factor and a mode comparable
608 to diesel exhaust seen in the Traffic factor.

609
610 **3.2 2-Step PMF-LR Analysis**

611 Figure S232 shows the results of the linear regression of the NSD data plotted against the
612 PM₁₀ 1st scores and again what is remarkable is the similarity between these regression
613 source profile correlation plots and both the factors derived in Beddows et al. (2015) and
614 those from the 2-step PMF-PMF analysis.

615

616 This PMF-LR analysis was carried out using daily averaged data and ~~to~~ to obtain hourly
617 information ~~and~~ and thus obtain the diurnal patterns (Figure S235) ~~and~~ the resulting regression
618 source profiles correlation factors were re-fitted to the original NSD data. On inspection of
619 these source profiles and diurnal plots, the negative values make interpretation a struggle
620 reinforcing one of the 4 conditions (Hopke, 1991) in the analysis if it is to make sense. We
621 can however fit non-negative gradients using non-negative regression. However, the
622 surprising consequence of applying this constraint is that the same profiles are derived but
623 they are clipped so that all negative values are replaced by zero values – hence, information
624 is lost by doing this. One interpretation of the negative values is that these are particle sinks
625 but this contradicts the PMF-PMF findings and hence it is concluded that the PMF-LR
626 analysis only serves as an indication of how the PM₁₀ factors are augmented by the NSD
627 data. If all profiles are shifted to above the zero line then comparisons to the PMF-PMF data
628 can be made. However, what is interesting to note in this result is the intercept NSD which
629 is comparable in profile and diurnal pattern to the nucleation mode identified in Beddows et
630 al. (2015). This is a seventh factor regression source profile, in addition to the 6 PM₁₀ factors
631 and suggests that although the PMF analysis of the PM₁₀ data alone misses a Nucleation
632 factor, this can be recovered in a second analysis as a remainder or bias in the data.
633 Furthermore, this result indicates that the composition of the Nucleation NSD factor has no
634 link to the chemical PM₁₀ composition and cannot be used to infer a composition. This is
635 unsurprising given the very small mass contributed by the nucleation mode particles.

636

637 Returning to the PMF-PMF analysis and extending the analysis from 6 factors to 7 factors,
638 and adding an extra row in the FKEY key matrix was added to which pulls all of the ¹G₇
639 scores contributions to ²F₇ to zero in the solution (Figure S12). The same FKEY matrix of
640 fkey₁ and 0 values was used but this time it was augmented with a 7th row of fkey₂ and zero

641 values. In this case, the $fkey_2$ values were set to a value of 20.

642

643 The same 6 factor solution is obtained with the additional 7th factor (Figure 4 and Figure
644 S334) and, As expected, this seventh factor was a Nucleation factor. It was suspected
645 that in the 6 factor solution, the ~~n~~Nucleation factor was combined with the Fuel-Oil factor.
646 This does not suggest any link between the ~~n~~Nucleation and Fuel-Oil factor other than there
647 ~~were~~ was an insufficient number of factors within the model for the two to factorise out of
648 the data giving the Fuel-Oil NSD profile a more reasonable modal peak between 50 and 60
649 nm rather than ~~20, 30~~ and 60 nm.

650

651 In the results of Beddows et al. (2015), applied a 1-step analysis to three different datasets:
652 PM₁₀-only; NSD-only and PM₁₀+NSD. The analyses of the PM₁₀-only and NSD-only – both
653 with homogenieous units - produced quantitative timeseries G. This was unlike the analysis
654 of the PM₁₀+NSD with heterogenieous units which could not apportion its 5 factors using G
655 but was able to factorise out a the-Nucleation factor from the data, seen also in the 4 sources
656 in the PMF solution for the NSD-only data. ~~was only seen when applying PMF to the just-~~
657 NSD and PM₁₀+NSD data, and in the PM₁₀+NSD results, ~~Fuel Oil was not separated and~~
658 appeared to be smeared across all 5 factors. A PM₁₀-only seven factor solution ~~to PMF of~~
659 the ~~PM₁₀ chemical composition data~~ did not reveal this factor either, presumably because
660 the mass associated with nucleation mode particles is too small to affect composition
661 significantly. Furthermore, Fuel Oil was not factorised out of the PM₁₀+NSD data and was
662 more likely divided across all 5 factors.

663

664 Another interesting observation is that although only 4 factors were derived from the PMF

665 analysis of NSD ~~data~~ alone (Diffuse Urban; Secondary; Traffic and Nucleation), when extra
666 information is included from the PMF analysis of the PM₁₀ data, more information can be
667 extracted from the PMF analysis of the NSD data in the form of the Marine; Fuel Oil and
668 NET & Crustal factors. The Nucleation factor is only revealed when performing a regression
669 between the NSD size bins and the G scores of the PM₁₀ PMF analysis which leads to
670 increasing the factor number from 6 to 7 which yields the Nucleation profile. It is also
671 reassuring that the bivariate plots for ~~of~~ the 7 factors (discussed in the next section)
672 correspond to the bivariate plots given in Beddows et al. (2015). Also note, that there is no
673 reason why any further investigation might not explore using more than 7 factors. In fact
674 the ~~n~~Nucleation factor appears at first glancesight to be multimodal. However, we restricted
675 our analysis to 7 factors, considering it complete in terms of identifying the sources obtained
676 by Beddows et al. (2015).

677

678 3.3 Diurnal and Bivariate Plots

679 The original PMF was carried out on daily PM₁₀ data and in order to make diurnal and
680 bivariate plots, a higher time resolution is ~~required~~desirable. It is assumed that the factors
681 derived in the hourly NSD data are the same as those derived from the daily averaged data,
682 i.e. the factors are conserved when averaging the data from hourly to daily data before PMF
683 analysis. Then the hourly NSD data can be fit with the PMF profiles derived from the daily
684 data (see Section 2.54). Figure 5 shows the resulting diurnal profiles. The diurnal trends of
685 the parameter c_k (equation 447), required fitted peaks show the values required in equation
686 3 to fit the 7 daily NSD factors to the hourly NSD data are shown. These have been scaled
687 to PN (measured in 1/cm³) in these plots according to using the integral of the NSD (equation
688 128) factor measured in 1/cm³. The ~~n~~Nucleation factor diurnal trend behaves as expected
689 rising to a maximum during the day and then falling back down to a minimum at night. This

690 corresponds to the intensity of the sun during the day and the increased likelihood of
691 nucleation on clean days when there is sufficient precursor material to form particles with a
692 low particle condensation sink. The Marine factor is also high during the day presumably
693 due to higher wind speeds. Diffuse Urban, NET and & Crustal, and Traffic all follow a trend
694 which is synchronised to the daily cycle of anthropogenic activity and traffic as influenced by
695 greater atmospheric stability at night. The Secondary factor shows a small diurnal range.
696 ~~also follows a similar anthropogenic cycle, however, although the polar plots are comparable~~
697 ~~to the and would be expected to be strongest at night those of Beddows et al 2015, the~~
698 ~~nighttime contributions is small. This results a contribution not being strong during the night~~
699 ~~in the diurnal trend plot of Figure 5 as would be expected when compared to the NSD diurnal~~
700 ~~trend of Beddows et al 2015.~~ Fuel Oil is highest during the evening and night and may
701 correspond to home heating rather than marine shipping emissions activity. The particle size
702 distributions associated with the Marine and NET and & Crustal sources are of limited value
703 as these sources are dominated by coarse particles, beyond the range of the SMPS data,
704 although there is a sharp increase in the volume of the particles above 0.5 μm in the Marine
705 factor. As pointed out in Beddows et al. (2015), ~~the mMarine factor is interesting by way of~~
706 ~~the fact that we would indeed expect to see the wing of a coarse particle mode, whose modal~~
707 ~~diameter is way above the upper size bin of the SMPS and in the coarse mode.~~ Instead,
708 the factor is identified by its chemical profile of sodium and chloride and is accompanied by
709 an aged nucleation mode at around 30nm. This can be either viewed simply as clean marine
710 air being 'polluted' by traffic emission and/or as the consequence of nucleation occurring over
711 at city for in a clean maritime air masses (Brines et al. 2015). The key point here is that the
712 factors derived in this work are comparable to those factorised in Beddows et al. (2015)
713 using the combined data-set and the advantage of the 2-step approach is that now we have
714 quantified hourly timeseries G.

715

716 The hourly contributions are aggregated into daily values and plotted as bivariate plots in
717 Figure 57 to assist comparison with the daily plots in Beddows et al. (2015). In that work,
718 the same PMF analysis of the NSD data yielded 4 factors which are ~~represented here~~
719 ~~again named identically to those~~ in the bivariate plots. The similarity of both of the polar and
720 annular plots for each of the 4 factors ~~justifies supports~~ our ~~aformentioned previous~~ factor-
721 ~~fitting assumption identification~~. The Secondary and Diffuse Urban are background sources
722 with strongest contributions in the evening and morning. Traffic is strongest for all wind
723 speeds from the East which makes sense since North Kensington is to the West of the city
724 centre of London where traffic is expecting to be most dense. Nucleation is also seen to be
725 strongest for those wind direction from the West which are expected to be cleaner, and have
726 a lower condensation sink. NET & Crustal and Fuel Oil are similar to Diffuse Urban
727 suggesting a similar predominant source location in the centre of London. Marine is
728 observed to be strongest for elevated wind speeds for all wind directions which is consistent
729 with the expected strong contribution for all high wind speeds from the South West, as
730 observed in the daily polar plots in Beddows et al. (2015).

731

732 3.4 Composition associated with ~~the Nucleation Hidden~~ Factor

733 The Nucleation factor was extracted from the two-step PMF-PMF analysis ~~when which~~
734 ~~included pulling the 1G_1 - 1G_6 to zero of factor 2F_7 . forcing the condition of no PM_{10} contribution~~
735 ~~through G_1 to G_6 .~~ It might be reasonable to suggest that if the two-step PMF-PMF analysis
736 is repeated and the order of analysis of PM_{10} and NSD datasets reversed that it would be
737 possible to derive the chemical conditions within the atmosphere which were conducive to
738 nucleation. For this, the time series of the 4 NSD factors (1G_1 - 1G_4) reported in Beddows et
739 al. (2015) were combined with the PM_{10} data. We again assume that the first PMF step has

740 been carried out and that we are satisfied with how the final solution represents the urban
741 environment of the receptor site and that there are no rotational ambiguities. We then carry
742 out the second step PMF analysis on the 34 x 591 input matrix ($^1G1...^1G4$,
743 $PM_{10}[PM, PM_{carbon}, PM_{ions}, PM_{metals}]$). The hourly output uncertainties from the first PMF
744 analysis of the NSD data $^1\Delta G1...^1\Delta G4$ were carried forward into the second PMF analysis
745 by adding them *in quadrature* to give daily uncertainties. As with the analysis of the auxillary
746 data in the PM_{10} -NSD data, the measurement uncertainties for the PM_{10} data (this time the
747 auxillary data) was naively taken as 4 times the PM_{10} matrix. Extra care could have been
748 take in assigning the PM_{10} uncertainties but since we force the output using FKEY a simpler
749 approach was taken. In fact, the FKEY consisted of a 4 x 4 diagonal matrix of zero values
750 with an $fkey_1$ of 20 for all the off-diagonal positions joined to a 4 x 30 matrix of zeros.
751 Furthermore, the uncertainty values of the PM_{10} were scaled until $Q/Q_{theory} = 0.99$ using
752 parameter $b_{scale} = 0.35$ (see Table S3 for more details).

753

754 Ideally, ~~for this~~ the chemical data would be ~~more informed with regards~~ limited to the
755 composition of the particles ~~below 100 nm (eg using $PM_{0.1}$ or $PM_{1.0}$) in the same size range~~
756 as the SMPS data. However, when since we are using the PM_{10} composition data we can
757 at best describe the composition of the aerosol which accompanied each factor (Figure
758 S45). For the NSD Secondary NSD-factor with its strongest contribution (indicated by the
759 Expected/Explained Variation) ~400 nm, we have a strong contribution to PM_{10} and $PM_{2.5}$
760 contribution together with nitrate, sulphate and ammonium. Diffuse Urban, with its strongest
761 contribution at 100 nm is accompanied by contributions ~~to~~ from elemental carbon and wood
762 smoke indicative of traffic and recreational wood burning. There ~~is~~ are also contributions from
763 barium, chromium, iron, ~~M~~ molybdenum, ~~A~~ antimony and ~~V~~ vanadium, all indicative of ~~non-~~
764 exhaust traffic emissions and the burning of fuel oil. Similarly, the ~~t~~ Traffic factor has a modal

765 ~~-diameter at roughly 30 nm which is indicative of exhaust emissions and this is accompanied~~
766 ~~by contributions to aluminum, barium, calcium, copper, iron, manganese, titanium and~~
767 ~~various other metals attributed to vehicles, albeit from tyre or brake wear or resuspension.~~
768
769 ~~For t~~The Nucleation factor ~~with its peak ~20 nm, this~~ was associated with marine air ~~with as~~
770 ~~indicated by the~~ strong contributions to Na, Cl and Mg (Figure S4S4). ~~—~~There are also
771 traces of V, Cr, Ni and a high ~~contribution to~~ PM₁₀ ~~level-mass~~ which are all associated with
772 marine air. This is explained by an association with the south-westerly wind sector which
773 brings strong winds and marine aerosol rather than reflecting the composition of the
774 nucleation particles themselves. ~~Marine air is considered to provide the conditions required~~
775 ~~of an air mass which is~~ conducive to nucleation, i.e. cleaner air with particles with a low
776 ~~condensation sink. As these air masses pass over the land and eventually into London,~~
777 ~~anthropogenic precursor gases are added to this air which then nucleate particles seen at~~
778 ~~the receptor site as a nucleation mode. This also goes some way to explain the earlier~~
779 ~~observation of aged nucleation particles observed in the marine factor in Figure S34. There~~
780 ~~are also strong contributisons to vanadium which is most likely from an un-resolved Fuel Oil~~
781 ~~source being mixed into the mMarine and eDiffuse uUrban factors. Secondary shows a~~
782 ~~strong association with ammonium, nitrate and sulphate but there are also traces of~~
783 ~~organics, Al, Cd, Mn, Pb, Ti and Zn and high PM_{2.5} and PM₁₀. Diffuse Urban makes the~~
784 ~~smallest contribution to PM but shows strong elemental carbon, wood smoke, Ba, Cr, Fe,~~
785 ~~Mo, Sb, V and Zn; indications of recreational wood burning and brake dust. Traffic has~~
786 ~~strong associations with Ba, Al, Ca, Cu, Mn, Ti and Zn which have sources in tyre and brake~~
787 ~~dust and resuspension.~~

788

789 4. CONCLUSIONS

790 ~~It is recommended when applying PMF to atmospheric PM data that only metrics with the~~
791 ~~same unit are input in order to make a meaningful quantitative apportionment. However, t~~
792 A two-step PMF analysis method is presented whereby existing PMF profiles can be extend
793 to incorporate auxillary data concurrently measured and having different units. This is
794 exemplified using PM₁₀ and NSD data.

795
796 When analysing PM₁₀ data, the inclusion of auxillary data such as meteorological, gas and
797 particle number data has proved to give a clearer separation of factors. However, for a
798 successful output, there must be no rotational ~~ambibuity~~ambiguity in either the PM₁₀ data or
799 in the auxillary data. In the ideal case, the individually computed factors G(X), G(Z) and
800 G(X,Z) need to be similar if the joint model is to be successful and not produce ~~te~~-large
801 residuals and hence a too large ~~a~~-Q value. In the best case, the total weight of the PM₁₀
802 data can be set higher than the auxillary data so that the PM₁₀ data drives the analysis. In
803 this work, we present an alternative method called the 2-step PMF method. Mixed unit
804 datasets limit the PMF to a qualitative analysis and the quantitative step of apportioning the
805 sources to a mass or number concentration has to be omitted. This problem is overcome in
806 this work by using a novel Two-Step PMF approach. In the first step the PM₁₀ data is PMF
807 analysed using the standard approach without the inclusion of additional data. An
808 appropriate solution is derived using the methods described in the literature in order to give
809 an initial separation of source factors. The time series G (and errors) of the PM₁₀ solution
810 are then taken forward into the second step where they are combined with the NSD data.
811 The PMF analysis is then repeated using the combined and mixed unit G time series and
812 NSD dataset. In order to ensure that unique factors are obtained for the G scores, Fkey
813 FKEY is used to pull off-diagonal values to zero thus driving the NSD data. This ensures
814 that the NSD factors are specific to the PM₁₀ solution and the PM₁₀ analysis is not affected

815 by any rotational ambiguity of the NSD data. For our demonstration using the Beddows et
816 al. (2015) analysis, this results in 6 PM₁₀ factors ~~which are not only~~ whose time series are
817 not only apportioned in mass but the source profiles are ~~augmented by~~ identified for the NSD
818 data. Comparisons of both the factor profiles, diurnal trends and bivariate plots to those of
819 Beddows et al. (2015), show that this technique produces one solution linking the two
820 separated solutions for PM₁₀ and NSD data datasets together. This generates confidence
821 that the NSD and PM₁₀ factors ascribed to one source are in fact attributable to that same
822 source.

823

824 Hence, the process starts with a dataset which produces a solution which is sensitive to
825 mass but the factors more sensitive to number can be accessed using a second step.
826 Furthermore, by exploring a higher number of factors, NSD factors which are insensitive to
827 PM₁₀ mass can be identified as in the case of the Nucleation factor. This information can
828 also be extracted using a linear regression PMF-LR where the size bins of the NSD data are
829 regressed against the PM₁₀ PMF time series. For this dataset, the Nucleation factor profile
830 is identified as an intercept within the fitted model leading to an increase in the number of
831 PMF factors from 6 to 7.

832

833 **5. ACKNOWLEDGEMENTS**

834 The National Centre for Atmospheric Science is funded by the U.K. Natural Environment
835 Research Council. Figures were produced using CRAN R and Openair (R Core Team, 2016;
836 Carslaw and Ropkins, 2012).

837

838

839 **REFERENCES**

- 840 [Beccaceci, S., Mustoe, C., Butterfield, D., Tompkins, J., Sarantaridis, D., Quincey, D.,](#)
841 [Brown, R., Green, D., Grieve, A., Jones, A.: Airborne Particulate Concentrations and](#)
842 [Numbers in the United Kingdom \(phase 3\), Annual Report 2011, NPL Report as 74, 2013a,](#)
843 [https://uk-](https://uk-air.defra.gov.uk/assets/documents/reports/cat05/1306241448_Particles_Network_Annual_Report_2011_(AS74).pdf)
844 [air.defra.gov.uk/assets/documents/reports/cat05/1306241448_Particles_Network_Annual](https://uk-air.defra.gov.uk/assets/documents/reports/cat05/1306241448_Particles_Network_Annual_Report_2011_(AS74).pdf)
845 [Report 2011 \(AS74\).pdf.](https://uk-air.defra.gov.uk/assets/documents/reports/cat05/1306241448_Particles_Network_Annual_Report_2011_(AS74).pdf)
846
847 [Beccaceci, S., Mustoe, C., Butterfield, D., Tompkins, J., Sarantaridis, D., Quincey, D.,](#)
848 [Brown, R., Green, D., Fuller, G., Tremper, A., Priestman, M., Font, A. F., Jones, A.: Airborne](#)
849 [Particulate Concentrations and Numbers in the United Kingdom \(phase 3\), Annual Report](#)
850 [2012, NPL Report as 74, 2013b, https://uk-](#)
851 [air.defra.gov.uk/assets/documents/reports/cat05/1312100920_Particles_Network_Annual](https://uk-air.defra.gov.uk/assets/documents/reports/cat05/1312100920_Particles_Network_Annual_report_2012_AS_83.pdf)
852 [report 2012 AS 83.pdf.](https://uk-air.defra.gov.uk/assets/documents/reports/cat05/1312100920_Particles_Network_Annual_report_2012_AS_83.pdf)
853
854 Beddows, D. C. S., Harrison, R. M., Green, D. C., and Fuller, G. W.: Receptor modelling of
855 both particle composition and size distribution from a background site in London, UK, *Atmos.*
856 *Chem. Phys.*, 15, 10107-10125, 2015.
857
858 ~~[Beddows, D. C. S., Dall'Osto, M., and Harrison, R. M.: An enhanced procedure for the](#)~~
859 ~~[merging of atmospheric particle size distribution data measured using electrical mobility and](#)~~
860 ~~[time-of-flight analysers, *Aerosol Sci. Technol.*, 44, 930-938 \(2010\).](#)~~
861
862 Bigi, A., and Harrison, R. M.: Analysis of the air pollution climate at a central urban
863 background site, *Atmos. Environ.*, 44, 2004-2012, 2010.
864
865 [Brines, M., Dall'Osto, M., Beddows, D. C. S., Harrison, R. M., Gómez-Moreno, F., Núñez, L.,](#)
866 [Artiñano, B., Costabile, F., Gobbi, G. P., Salimi, F., Morawska, L., Sioutas, C., and Querol,](#)
867 [X., Traffic and nucleation events as main sources of ultrafine particles in high-insolation](#)
868 [developed world cities, *Atmos. Chem. Phys.*, 15, 5929-5945, 2015.](#)
869
870 Carslaw, D. C. and Ropkins, K.: openair - an R package for air quality data analysis, *Environ.*
871 *Model Softw.* 27-28, 52-61, 2012.
872
873 [Cavalli, F., Viana, M., Yttri, K. E., Genberg, J., and Putaud, J.-P.: Toward a standardised](#)
874 [thermal-optical protocol for measuring atmospheric organic and elemental carbon: the](#)
875 [EUSAAR protocol, *Atmos. Meas. Tech.*, 3, 79-89, 2010.](#)
876
877 Chan, Y.-C., Hawas, O., Hawker, D., Vowles, P., Cohen, D. D., Stelcer, E., Simpson, R.,
878 Golding, G., and Christensen E.: Using multiple type composition data and wind data in
879 PMF analysis to apportion and locate sources of air pollutants, *Atmos. Environ.*, 45, 439-
880 449, 2011.
881
882 ~~[Comero, S., Capitani, L., and Gawlik, B. M.: Positive Matrix Factorisation \(PMF\) An](#)~~
883 ~~[introduction to the chemometric evaluation of environmental monitoring data using PMF,](#)~~
884 ~~[JRC Scientific and Technical Reports, 2009,](#)~~
885 ~~[https://pdfs.semanticscholar.org/24d3/7d67993228d05513f877b007a16d9a677ff0.pdf?ga](https://pdfs.semanticscholar.org/24d3/7d67993228d05513f877b007a16d9a677ff0.pdf?ga=2.219748825.1591505292.1532007606.1458741279.1523619082)~~
886 ~~[=2.219748825.1591505292.1532007606.1458741279.1523619082.](https://pdfs.semanticscholar.org/24d3/7d67993228d05513f877b007a16d9a677ff0.pdf?ga=2.219748825.1591505292.1532007606.1458741279.1523619082)~~
887

888 Contini D., Cesari D., Genga, A., Siciliano, M., Ielpo, P., Guascito, M. R., and Conte, M.: Source apportionment of size-segregated atmospheric particles based on the major water-
889 soluble components in Lecce (Italy), Sci. Tot. Environ., 472, 248-261, 2014.
890
891 Emami, F., and Hopke, P. K.: Effect of adding variables on rotational ambiguity in positive
892 matrix factorization solutions, Chemometr. Intell. Lab., 162, 198-202, 2017.
893
894 Fuller, G. W., Tremper, A. H., Baker, T. D., Yttri, K. E., and Butterfield, D.: Contribution of
895 wood burning to PM 10 in London, Atmos. Environ., 87, 87-94, 2014.
896
897 Harrison, R. M., Beddows, D. C. S., and Dall'Osto, M.: PMF analysis of wide-range particle
898 size spectra collected on a major highway, Environ.Sci.Technol., 45, 5522-5528, 2011.
899
900 Hopke, P. K.: A guide to Positive Matrix Factorization, J. Neuroscience, 2, 1-16, 1991.
901
902 Leoni, C., Pokorna, P., Hovorka, J., Masiol, M., Topinka J., Zhao, Y., Krupal, K., Cliff, S.,
903 Mikuska, P., and Hopke, P. K.: Source apportionment of aerosol particles at a European air
904 pollution hot spot using particle number size distributions and chemical composition,
905 Environ. Pollut., 234, 45-154, 2018.
906
907 Masiol, M., Hopke, P. K., Felton, H. D., Frank, B. P., Rattigan, O. V., Wurth, M. J., and
908 LaDuke, G. H.: Source apportionment of PM_{2.5} chemically speciated mass and particle
909 number concentrations in New York City, Atmos. Environ., 148, 215-229, 2017.
910
911 Norris, G., Duvall, R., Brown, S., and Bai, S.: EPA Positive Matrix Factorization (PMF) 5.0
912 Fundamentals and User Guide, U.S. Environmental Protection Agency, Washington, DC,
913 EPA/600/R-14/108 (NTIS PB2015-105147), 2014.
914
915 Ogulei, D., Hopke, P. K., Zhou, L., Pancras, J. P., Nair, N., and Ondov, J.M.: Source
916 apportionment of Baltimore aerosol from combined size distribution and chemical
917 composition data, Atmos. Environ., 40, S396-S410, 2006.
918
919 Paatero, P.: User's Guide to Positive Matrix Factorization Programs PMF2 and PMF3, Part
920 2, 2002.
921
922 Pant, P., and Harrison, R. M.: Critical review of receptor modelling for particulate matter: A
923 case study of India, Atmos. Environ., 49, 1-12, 2012.
924
925 Polissar, A. V., Hopke, P. K., and Paatero, P.: Atmospheric aerosol over Alaska – 2.
926 Elemental composition and sources, J. Geophys. Res.-Atmos., 103, 9045–19057, 1998,
927 doi:10.1029/98JD01212.
928
929 R Core Team. R: A language and environment for statistical computing. R Foundation for
930 Statistical Computing, Vienna, Austria, 2018. Available at: <https://www.r-project.org/>.
931
932 R Core Team. R: A language and environment for statistical computing. R Foundation for
933 Statistical Computing, Vienna, Austria, 2016. Available at: <https://www.R-project.org/>.
934
935 Sandradewi, J., Prevot, A. S. H., Weingartner, E., Schmidhauser, R., Gysel, M., and
936 Baltensperger, U.: A study of wood burning and traffic aerosols in an Alpine valley using a
937

938 [multi-wavelength Aethalometer, Atmos. Environ., 42, 101-112, 2008.](#)
939
940 [Sowlat M., H., Hasheminassab, S., and Sioutas, D.: Source apportionment of ambient](#)
941 [particle number concentrations in central Los Angeles using positive matrix factorization](#)
942 [\(PMF\), Atmos. Chem. Phys., 16, 4849-4866, 2016.](#)
943
944 Thimmaiah, D., Hovorka, J., and Hopke, P. K.: Source apportionment of winter submicron
945 Prague aerosols from combined particle number size distribution and gaseous composition
946 data, Aerosol Air Qual. Res., 9, 209-236, 2009.
947
948 Wang, X., Zong, Z., Tian, C., Chen, Y., Luo, C., Li, J., Zhang, G., and Luo, Y.: Combining
949 Positive Matrix Factorization and radiocarbon measurements for source apportionment of
950 PM_{2.5} from a national background site in north China, Sci. Rep., 7, 10648, 2017, doi:
951 10.1038/s41598-017-10762-8.
952
953 Wiedensohler, A., Birmili, W., Nowak, A., Sonntag, A., Weinhold, K., Merkel, M., Wehner,
954 B., Tuch, T., Pfeifer, S., Fiebig, M., Fjaraa, A. M., Asmi, E., Sellegri, K., Depuy, R., Venzac,
955 H., Villani, P., Laj, P., Aalto, P., Ogren, J. A., Swietlicki, E., Williams, P., Roldin, P., Quincey,
956 P., Hüglin, C., Fierz-Schmidhauser, R., Gysel, M., Weingartner, E., Riccobono, F., Santos,
957 S., Gruning, C., Faloon, K., Beddows, D., Harrison, R. M., Monahan, C., Jennings, S. G.,
958 O'Dowd, C. D., Marinoni, A., Horn, H.-G., Keck, L., Jiang, J., Scheckman, J., McMurry, P.
959 H., Deng, Z., Zhao, C. S., Moerman, M., Henzing, B., de Leeuw, G., Loschau, G., and
960 Bastian S.: Mobility particle size spectrometers: Harmonization of technical standards and
961 data structure to facilitate high quality long-term observations of atmospheric particle
962 number size distributions, Atmos. Meas. Tech., 5, 657-685, 2012.
963
964

965 **FIGURE LEGENDS:**

966

967 **Figure 1.** Venn Diagram showing the summary of the findings of Beddows et al. (2015);
968 applying PMF to PM₁₀-only, NSD-only and PM₁₀+NSD datasets. Table shows the
969 apportionment of PM₁₀ and NSD taken from Beddows et al. (2015).

970

971 **Figure 2.** Flow diagram showing the flow of data through the 2-step PMF-PMF analysis.
972 The PMF analyses of single data set X are considered in step 1 and output indicated by
973 factors/uncertainties ¹G, ¹ΔG, ¹F and ¹ΔF. The second PMF analysis is carried out on the
974 joint data set [¹GZ] and yields factors/uncertainties ²G, ²ΔG, ²F and ²ΔF. In our analysis,
975 X and ¹G are the PM₁₀ and resulting time series from the analysis of Beddows et al. (2015)
976 and Z is the auxillary NSD data concurrently measured using a SMPS.

977

978 **Figure 3.** Source profiles ¹F and ²F from both the first and second PMF step using 6
979 factors. [Grey bars and black line indicates the values of F; red lines and dots indicated
980 the explained variations; and grey dotted line indicates the dV/dlogDp.]

981

982 **Figure 4.** Nucleation and Fuel Oil factors derived when extending the second PMF analysis
983 from the 6 factors (shown in Figure 3) to allow for a 7th factors. Source profiles ²F₁ to ²F₆ are
984 given in Figure S34. Each plot is divided into 2 showing the output ¹F_k and ²F_k. [Grey bars
985 and black line indicates the values of F; red lines and dots indicated the explained variations;
986 and grey dotted line indicates the dV/dlogDp.]

987

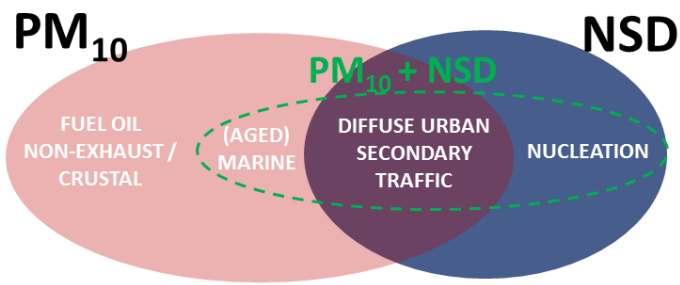
988 **Figure 5.** Diurnal cycles derived PN_k calculated by the fitting of the daily PMF factor profiles
989 to the hourly NSD data fitted (see equation 42-8 and sSection 2.54). [Left-left column –
990 diurnal trends of PN_k ; left-middle column – bivariate plot of PN_k ; middle-right – annular plot
991 PN_k ; right-right – bivariate plot of PN_k , plotted using the Openair program. Polar plots show
992 a point coloured according to the key, the number concentration at that point on the plot
993 whose distance from the origin represents wind speed and angle wind direction. Likewise
994 for the angular plots the number concentration represent wind direction at an hour of the day
995 between 0 and 23 hrs.]. Note that the diurnal plots do not start at zero.

996

997

998

999
1000



	PM ₁₀ [µg/m ³]	NSD [1/cm ³]
<u>Urban</u>	<u>4.1</u>	<u>2370</u>
<u>BackgroundDiffuse</u>		
<u>Urban</u>		
<u>Marine</u>	<u>2.6</u>	<u>-</u>
<u>Secondary</u>	<u>4.4</u>	<u>243</u>
<u>NET / Crustal</u>	<u>4.3</u>	<u>-</u>
<u>Fuel Oil</u>	<u>1.0</u>	<u>-</u>
<u>Traffic</u>	<u>0.8</u>	<u>2460</u>
<u>Nucleation</u>	<u>-</u>	<u>430</u>
<u>Total</u>	<u>17.2</u>	<u>5512</u>

Figure 1. Venn Diagram showing the summary of the findings of Beedows et al. (2015); applying PMF to PM₁₀-only, NSD-only and PM₁₀+NSD datasets. Table shows the apportionment of PM₁₀ and NSD taken from Beedows et al. (2015).

1001

1002

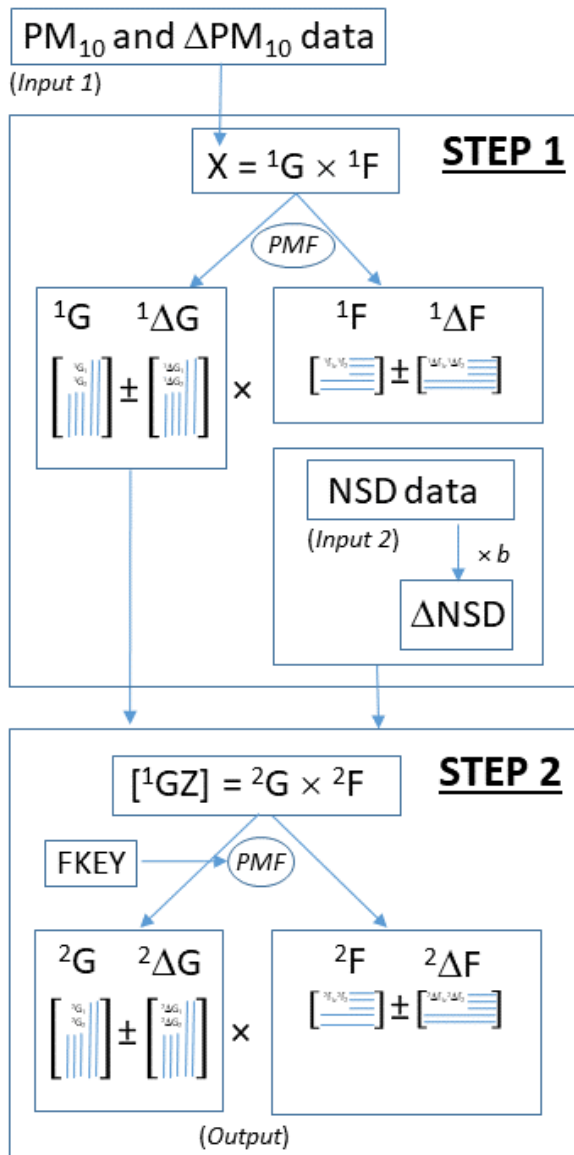
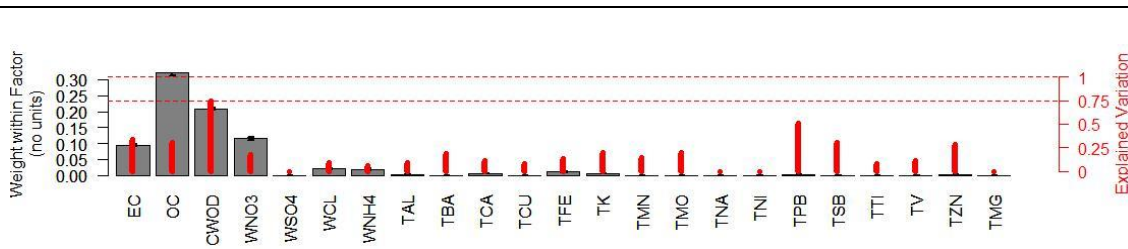


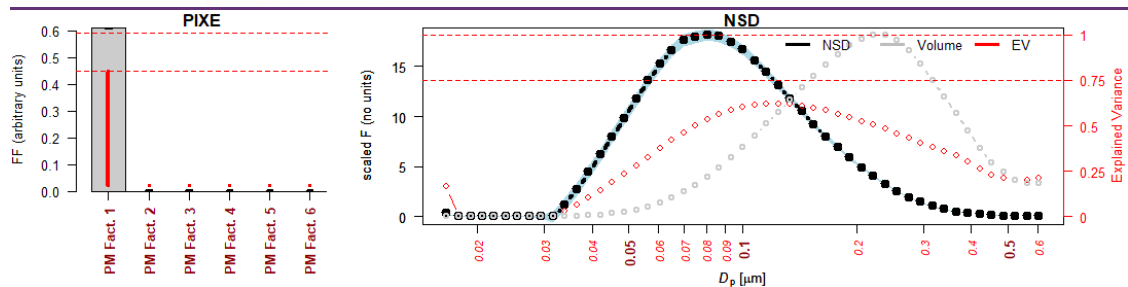
Figure 2. Flow diagram showing the flow of data through the 2-step PMF-PMF analysis. The PMF analyses of single data set X are considered in step 1 and output indicated by factors/uncertainties 1G , ${}^1\Delta G$, 1F and ${}^1\Delta F$. The second PMF analysis is carried out on the joint data set $[{}^1GZ]$ and yields factors/uncertainties 2G , ${}^2\Delta G$, 2F and ${}^2\Delta F$. In our analysis, X and 1G are the PM_{10} and resulting time series from the analysis of Beddows et al. (2015) and Z is the auxiliary NSD data concurrently measured using a SMPS.

Diffuse Urban

$1F_1$

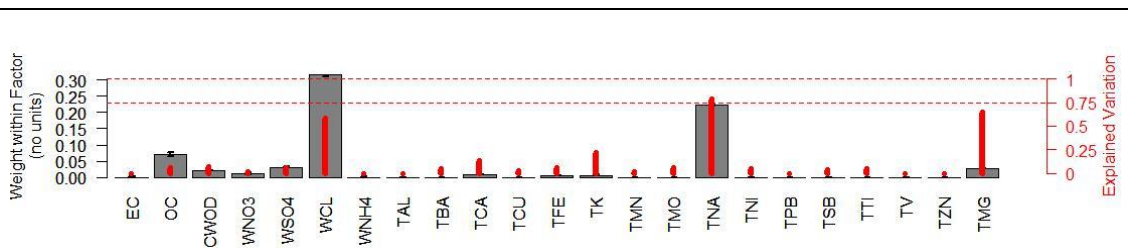


$2F_1$

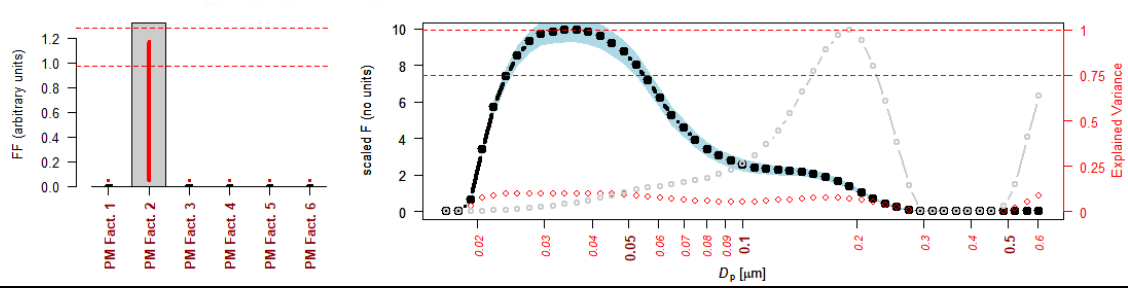


Marine

$1F_2$

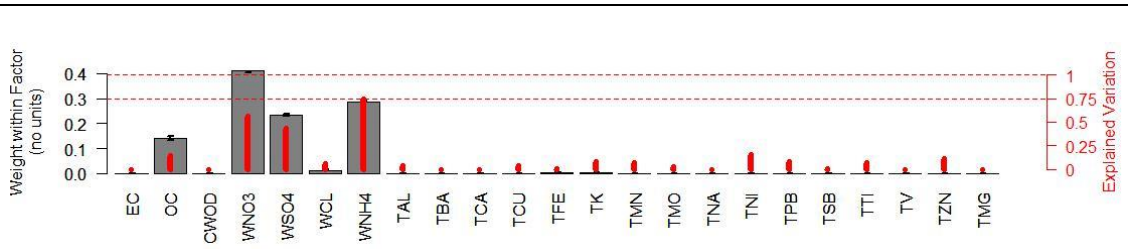


$2F_2$

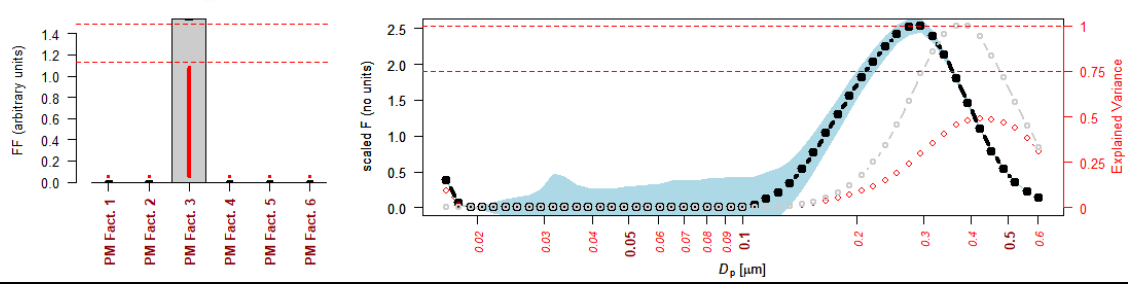


Secondary

$1F_3$



$2F_3$



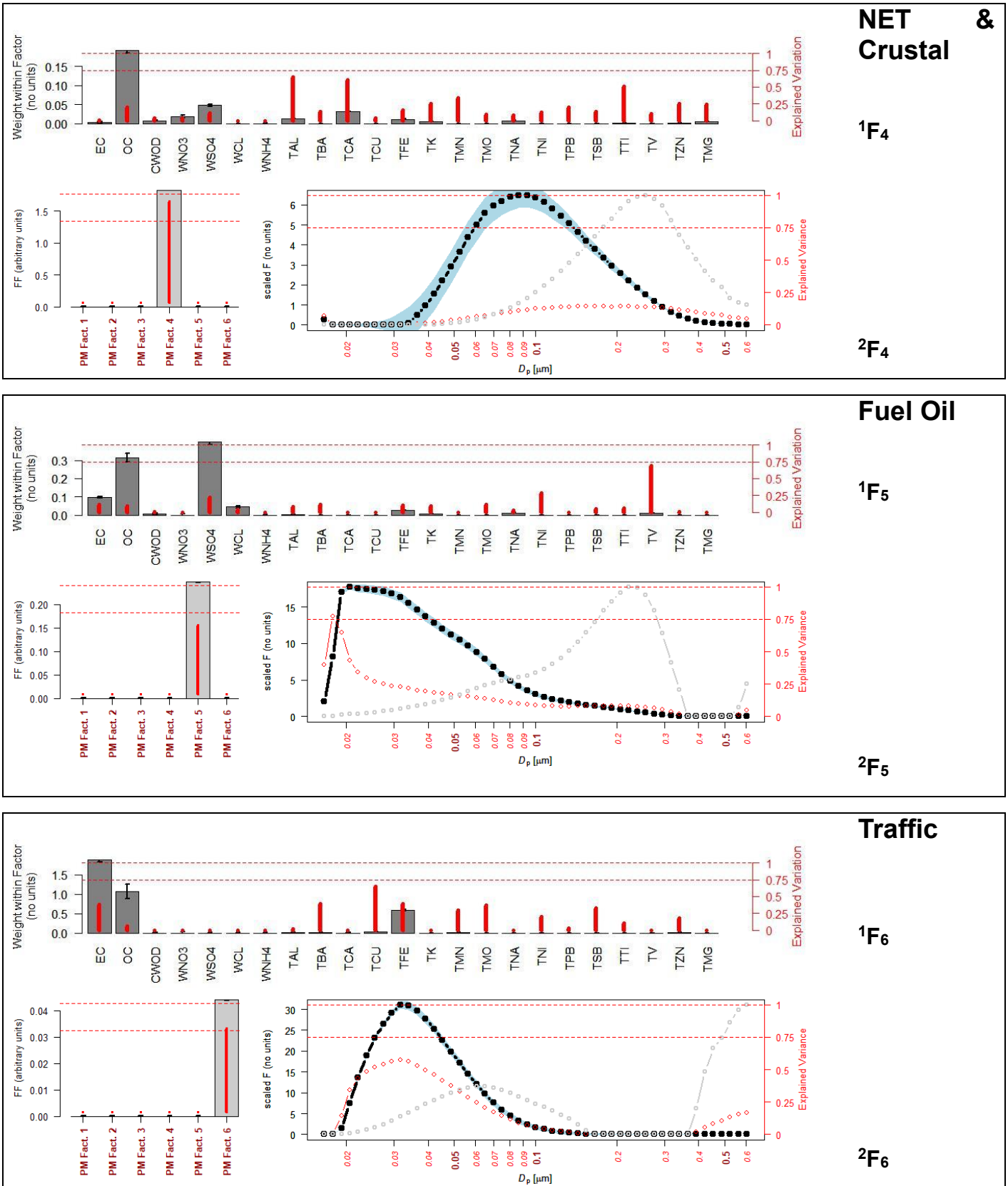


Figure 3. Source profiles 1F and 2F from both the first and second PMF step using 6 factors. [Grey bars and black line indicates the values of F; red lines and dots indicated the explained variations; and grey dotted line indicates the $dV/d\log D_p$.]

1008
1009
1010

1011
1012
1013

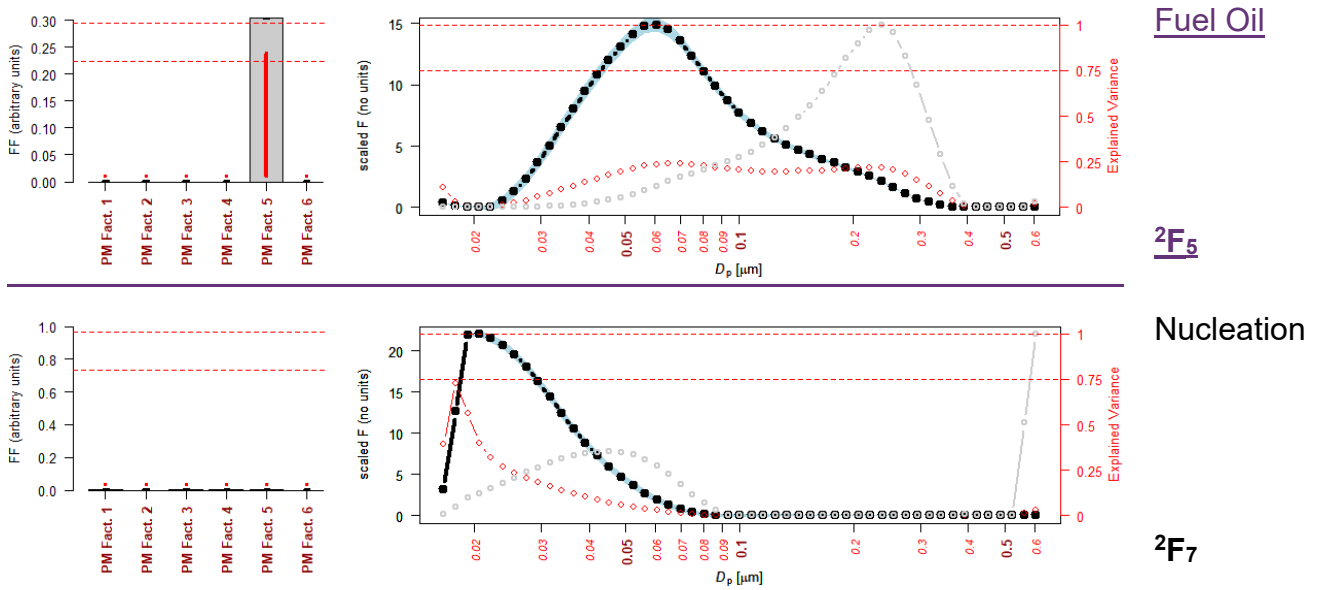


Figure 4. Nucleation and Fuel Oil factors derived when extending the second PMF analysis from the 6 factors (shown in Figure 3) to allow for a 7th factors. Source profiles 2F_1 to 2F_6 are given in Figure S34. Each plot is divided into 2 showing the output 1F_k and 2F_k . [Grey bars and black line indicates the values of F; red lines and dots indicated the explained variations; and grey dotted line indicates the $dV/d\log D_p$.]

1014
1015
1016
1017

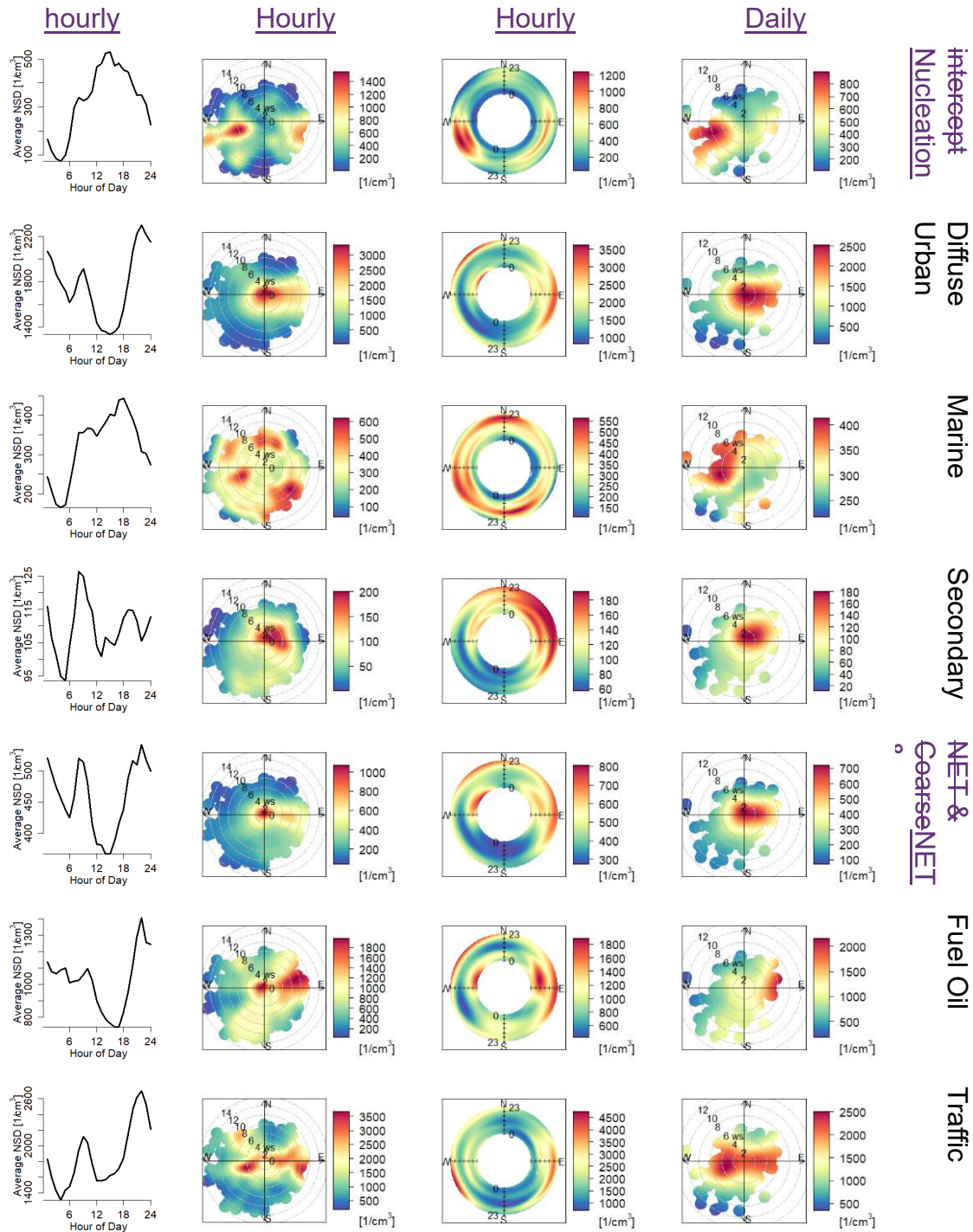


Figure 5. Diurnal cycles derived PN_k calculated by the fitting of the daily PMF factor profiles to the hourly NSD data fitted (see equation 12-8 and Section 2.54). [Left-left column – diurnal trends of PN_k ; left-middle column – bivariate plot of PN_k ; middle-right – annular plot PN_k ; right-right – bivariate plot of PN_k , plotted using the Openair program. Polar plots show a point coloured according to the key, the number concentration at that point on the plot whose distance from the origin represents wind speed and angle wind direction. Likewise for the angular plots the number concentration represent wind direction at an hour of the day between 0 and 23 hrs.]. Note that the diurnal plots do not start at zero.

1
2
3
4
5
6
7
8
9
10
11
12
13
14
15
16
17
18
19
20
21
22
23
24
25
26
27
28
29
30
31
32
33
34
35
36
37
38

SUPPLEMENTARY INFORMATION

RECEPTOR MODELLING OF BOTH PARTICLE COMPOSITION AND SIZE DISTRIBUTION FROM A BACKGROUND SITE IN LONDON, UK – THE TWO STEP APPROACH

David C.S. Beddows and Roy M. Harrison

39 **Table S1.** Setup of TSI SMPS.

40

EC 3080		
Neutraliser	Kr-85 radioactive source	
Drier	✓ EUSAAR/ACTRIS Drier	
DMA	TSI 3081 long DMA	
Aerosol Flow	0.3 lpm	
Sheath Flow	3.0 lpm	
Impactor Type	0.0508 cm	
HV Polarity	Neg	
AIM version	9.0	
Scans per Sample	6	
Number of Samples	1	
Total Sample Time	14 min 0 sec	
Multiple charge	✓	
Diffusion loss correction	✓	
Particle Density	1.2 g/cc	
Gas Density	0.0012 g/cc	
Nano Aggregate Mobility Analysis	✗	
<u>CPC3775</u>		
<u>CPC3775</u> Inlet flow	0.3 lpm	
Data Coverage	72.5 % over the 2 years 2011/2012	
Service and Calibration Date	February 2011 and February/March 2012	

41

42

43 **Table S2.** Miscellaneous PMF-PMF details for the PM₁₀-NSD data set.

44

INPUT DATA	(¹ G1... ¹ G6, NSD ₁ ^{16nm} ...NSD ₅₂ ^{640nm})
<i>Input Settings</i>	
PMF2 version number	4.2
Number of Factors	6
FPEAK	0.1
Input dimensions: Row x Columns	590 x 58
Number of Repeats	1
Outlier Distance	4
Robust Analysis	✓
Error Model	-12
Seed	3
Initially Skipped	0
Uncertainty Matrices T/U/V	✓/✗/✗
Normalization of factor vectors before output	None
Optional parameter lines	missingneg 10
<i>Output values</i>	
Q in the robust mode	30333
Q when not down weighting outliers	32568
POS-Outlier limit (4.0) exceeded by	221 positive residuals
NEG-Outlier limit (4.0) exceeded by	38 negative residuals

45

46
47
48

Table S3. Miscellaneous PMF-PMF details for the NSD-PM₁₀ data set.

INPUT DATA	([¹ G1... ¹ G4],PM ₁₀ [PM,PM _{carbon} ,PM _{ions} ,PM _{metals}]).
<i>Input Settings</i>	
PMF2 version number	4.2
Number of Factors	4
FPEAK	0.1
Input dimensions: Row x Columns	591 x 34
Number of Repeats	1
Outlier Distance	4
Robust Analysis	✓
Error Model	-12
Seed	3
Initially Skipped	0
Uncertainty Matrices T/U/V	✓/x/x
Normalization of factor vectors before output	None
Optional parameter lines	missingneg 10
<i>Output values</i>	
Q in the robust mode	17652
Q when not down weighting outliers	18089
POS-Outlier limit (4.0) exceeded by	19 positive residuals
NEG-Outlier limit (4.0) exceeded by	3 negative residuals

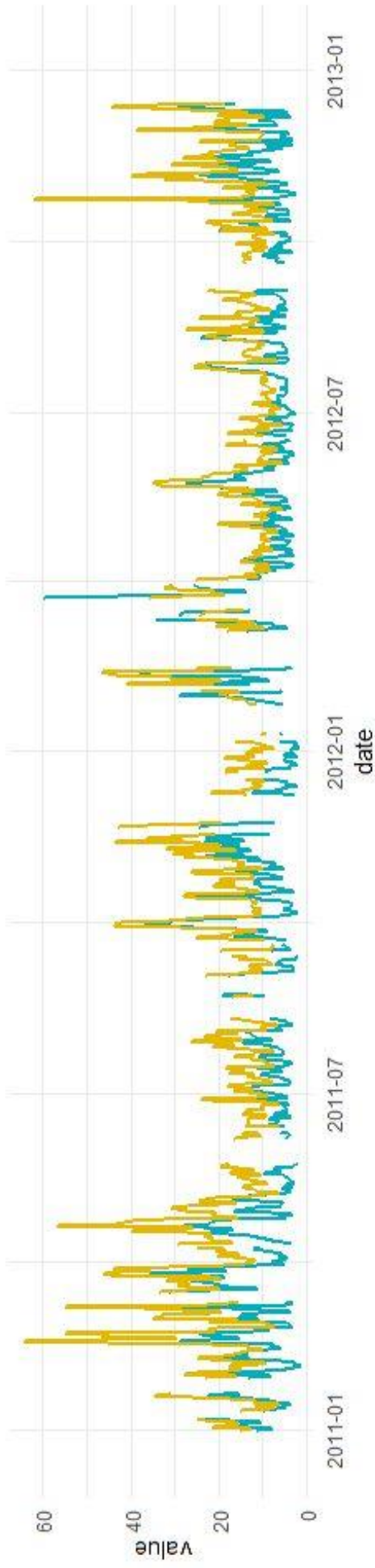
49
50
51

Table S4. Summary of the regression results, comparing ¹G_k with ²G_k for *k* in 1 to 6.

		<i>const</i> in ¹ G _k = <i>const</i> x ² G _k	R ²
Diffuse Urban	¹ G ₁ vs ² G ₁	1.2	0.72
Marine	¹ G ₂ vs ² G ₂	0.73	0.94
Secondary	¹ G ₃ vs ² G ₃	0.56	0.71
NET & Crustal	¹ G ₄ vs ² G ₄	0.54	0.96
Fuel Oil	¹ G ₅ vs ² G ₅	2.9	0.41
Traffic	¹ G ₆ vs ² G ₆	15.5	0.40

52
53
54
55
56
57
58
59
60
61

— PM[0.9] estimated from NSD — Sum of PMF apportionment



4

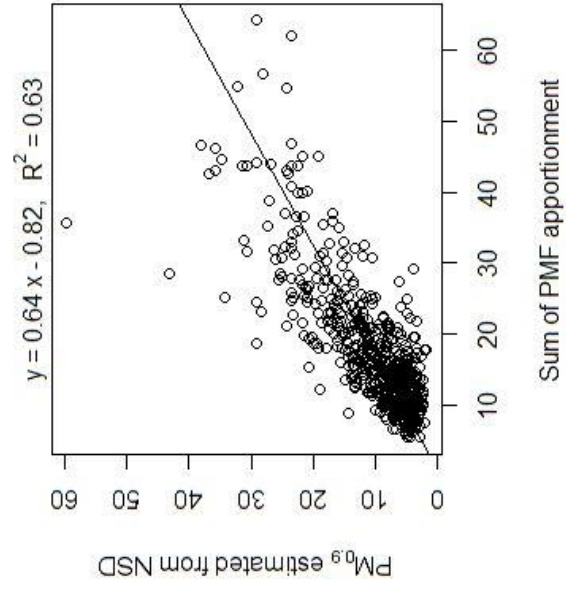


Figure S1. Plot of total apportioned PM₄₀ mass against PM_{0.9} mass estimated using the NSD data.

		<i>G</i> Time Series from Step 1						Number Size Distribution (nm)				
		¹ G1	¹ G2	¹ G3	¹ G4	¹ G5	¹ G6	16.6	17.8	19.2	⋮	604
Factors from Step 2	² F ₁	0	<i>fkey</i> ₁	0	0	0		0				
	² F ₂	<i>fkey</i> ₁	0	<i>fkey</i> ₁	<i>fkey</i> ₁	<i>fkey</i> ₁	<i>fkey</i> ₁	0	0	0		0
	² F ₃	<i>fkey</i> ₁	<i>fkey</i> ₁	0	<i>fkey</i> ₁	<i>fkey</i> ₁	<i>fkey</i> ₁	0	0	0		0
	² F ₄	<i>fkey</i> ₁	<i>fkey</i> ₁	<i>fkey</i> ₁	0	<i>fkey</i> ₁	<i>fkey</i> ₁	0	0	0		0
	² F ₅	<i>fkey</i> ₁	<i>fkey</i> ₁	<i>fkey</i> ₁	<i>fkey</i> ₁	0	<i>fkey</i> ₁	0	0	0		0
	² F ₆	<i>fkey</i> ₁	<i>fkey</i> ₁	<i>fkey</i> ₁	<i>fkey</i> ₁	<i>fkey</i> ₁	0	0	0	0		0

		<i>G</i> Time Series from Step 1						Number Size Distribution (nm)				
		¹ G1	¹ G2	¹ G3	¹ G4	¹ G5	¹ G6	16.6	17.8	19.2	⋮	604
Factors from Step 2	² F ₁	0	<i>fkey</i> ₁	0	0	0		0				
	² F ₂	<i>fkey</i> ₁	0	<i>fkey</i> ₁	<i>fkey</i> ₁	<i>fkey</i> ₁	<i>fkey</i> ₁	0	0	0		0
	² F ₃	<i>fkey</i> ₁	<i>fkey</i> ₁	0	<i>fkey</i> ₁	<i>fkey</i> ₁	<i>fkey</i> ₁	0	0	0		0
	² F ₄	<i>fkey</i> ₁	<i>fkey</i> ₁	<i>fkey</i> ₁	0	<i>fkey</i> ₁	<i>fkey</i> ₁	0	0	0		0
	² F ₅	<i>fkey</i> ₁	<i>fkey</i> ₁	<i>fkey</i> ₁	<i>fkey</i> ₁	0	<i>fkey</i> ₁	0	0	0		0
	² F ₆	<i>fkey</i> ₁	<i>fkey</i> ₁	<i>fkey</i> ₁	<i>fkey</i> ₁	<i>fkey</i> ₁	0	0	0	0		0
	² F ₇	<i>fkey</i> ₂	<i>fkey</i> ₂	<i>fkey</i> ₂	<i>fkey</i> ₂	<i>fkey</i> ₂	<i>fkey</i> ₂	0	0	0		0

Figure S2S1. Entries in the FKEY matrix used in step 2 of the PMF-PMF analysis using (a) 6 factors and (b) 7 factors. An extremely strong value of 24 was chosen for *fkey*₁ and 20 for *fkey*₂.

62
63
64

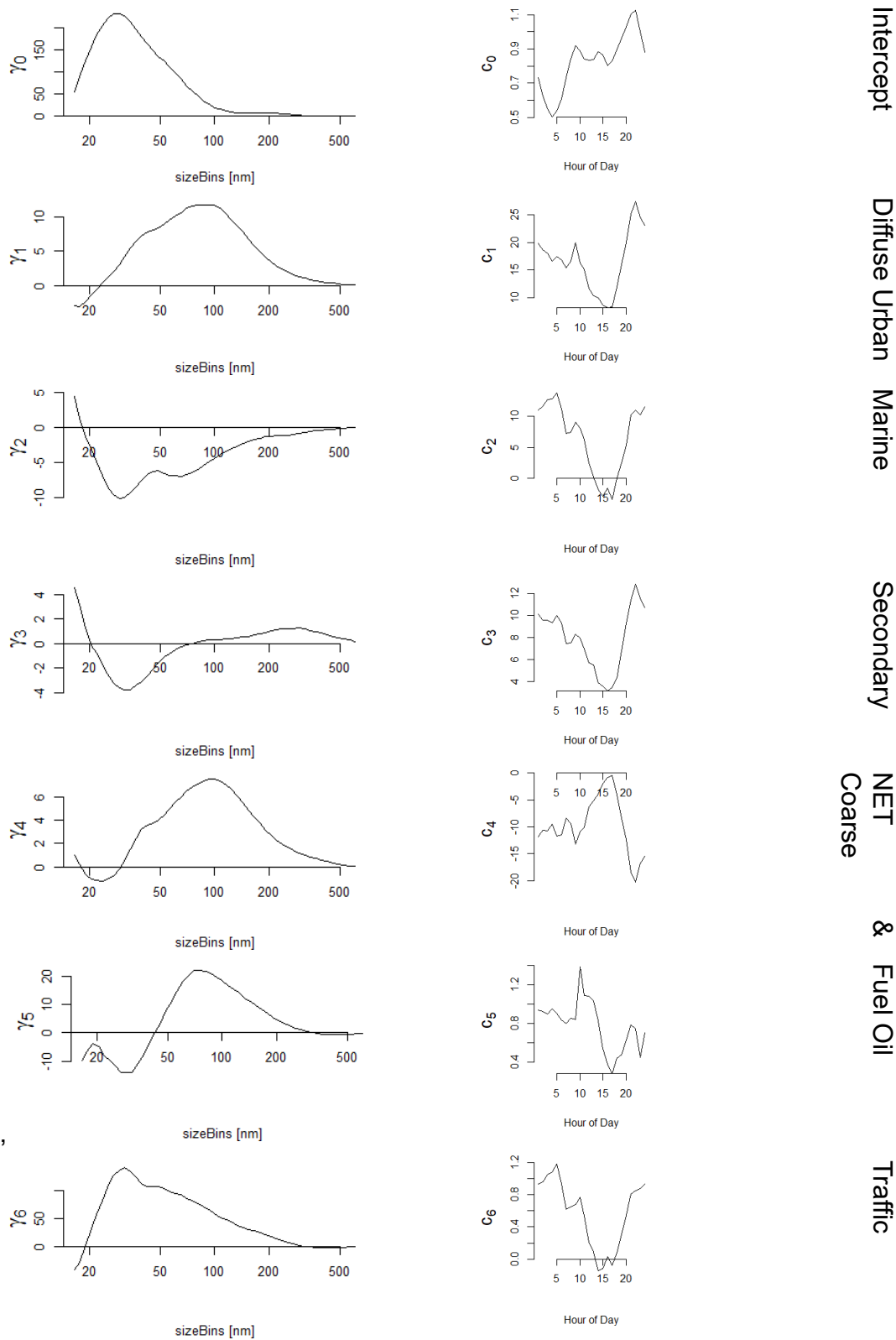
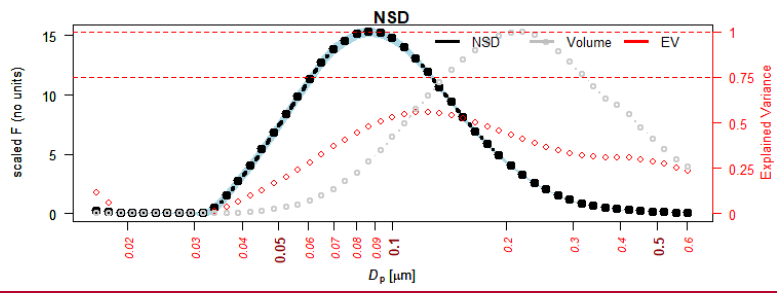
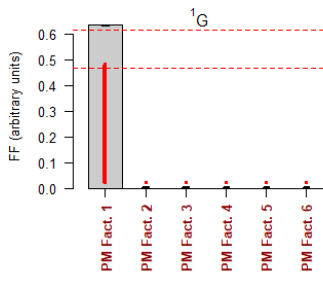
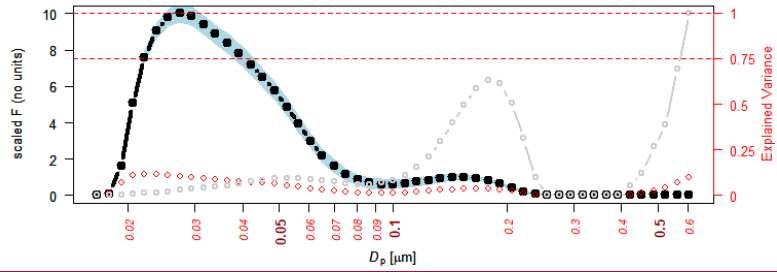
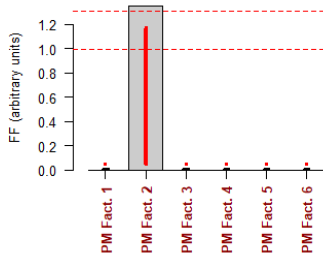


Figure S3S2. Daily regression source profiles (γ_k vs d_p in equation 8) obtained from regressing the NSD data against 1G_k (left hand panels) as in equation 4 and diurnal trends of the fit parameter c_k resulting from the fit of the daily regression source profiles to the hourly NSD data (equations 10 & 11).



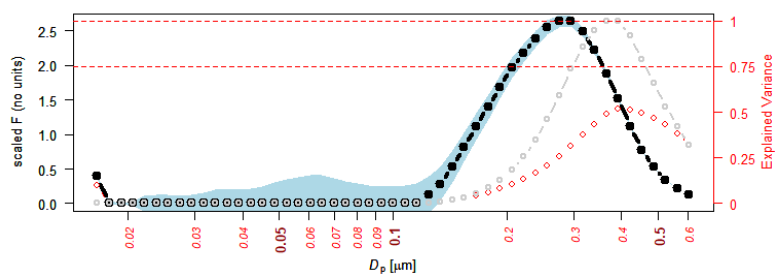
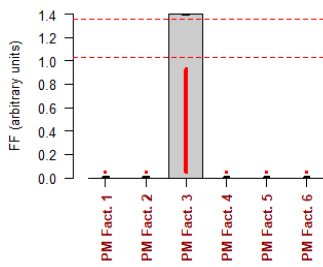
Diffuse Urban

2F_1



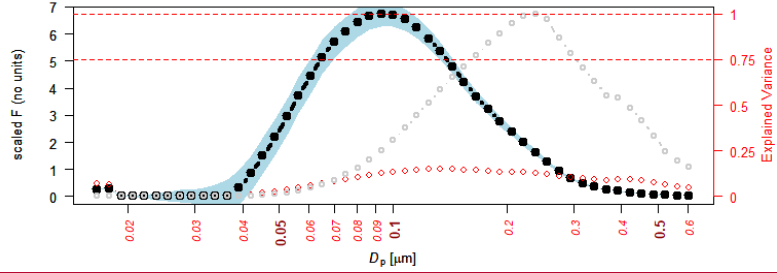
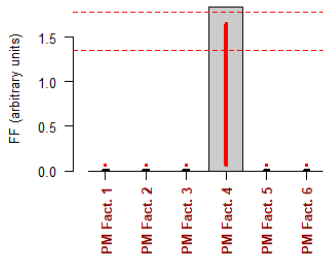
Marine

2F_2



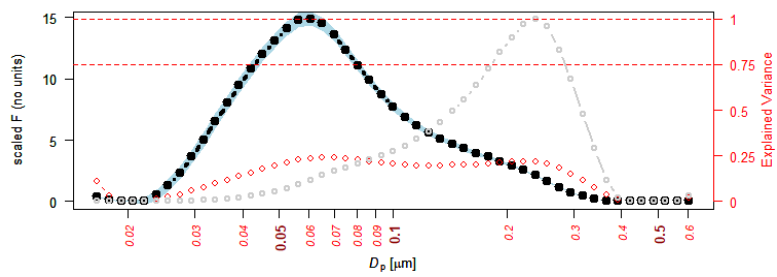
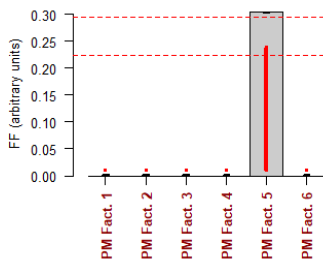
Secondary

2F_3



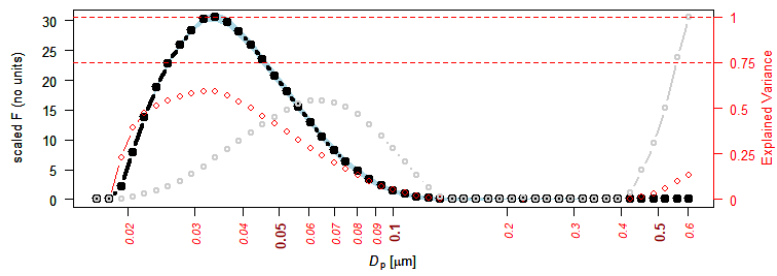
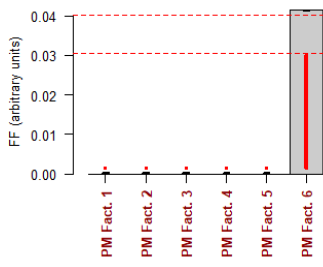
NET & Coarse

2F_4



Fuel Oil

2F_5



Traffic

2F_6

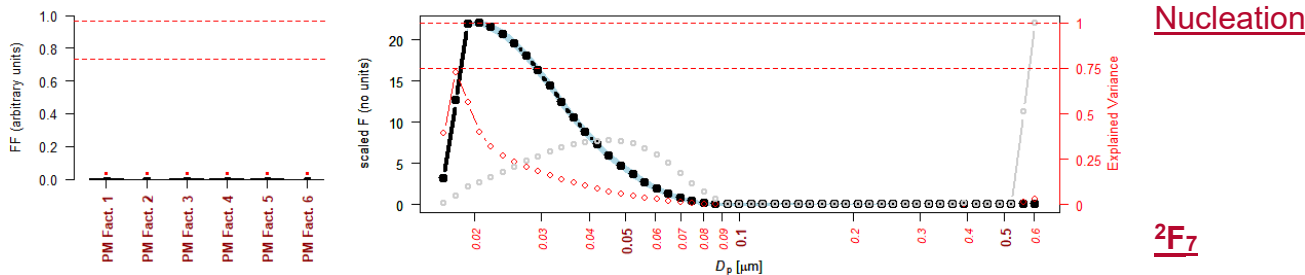


Figure S3. Source profiles 1F and 2F from both the first and second PMF step using 7 factors. [Grey bars and black line indicates the values of F ; red lines and dots indicated the explained variation; and grey dotted line indicates the $dV/d\log D_p$.]

67
68
69
70

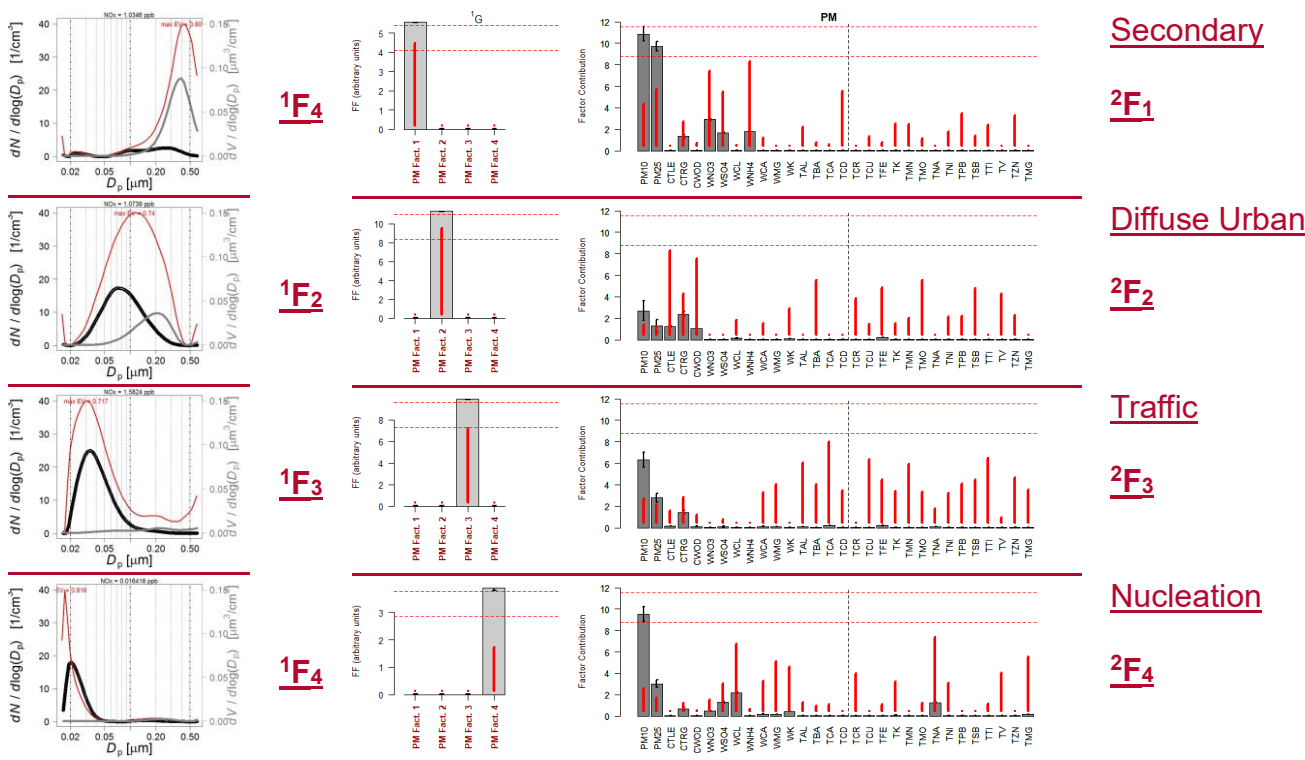
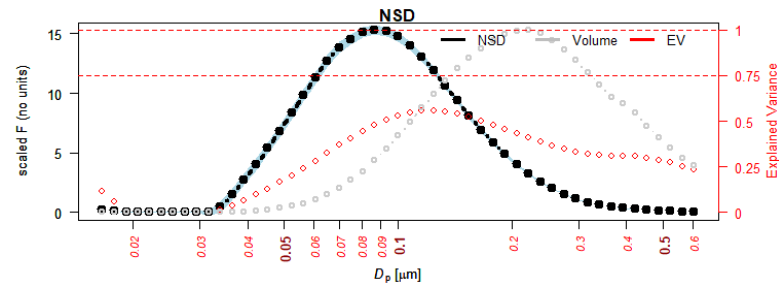
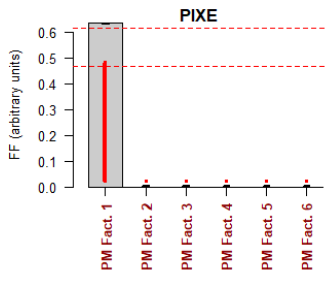


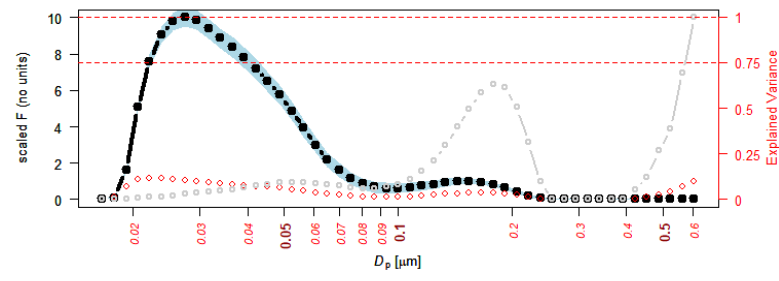
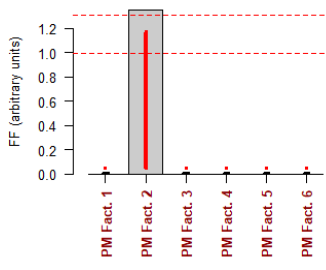
Figure S4. PMF-PMF 4 factor analysis of NSD data followed by PM_{10} . Each plot is divided into 2 showing the output 1F_k and 2F_k . [Grey bars and black line indicates the values of F ; red lines and dots indicated the explained variation; and grey dotted line indicates the $dV/d\log D_p$.]

71



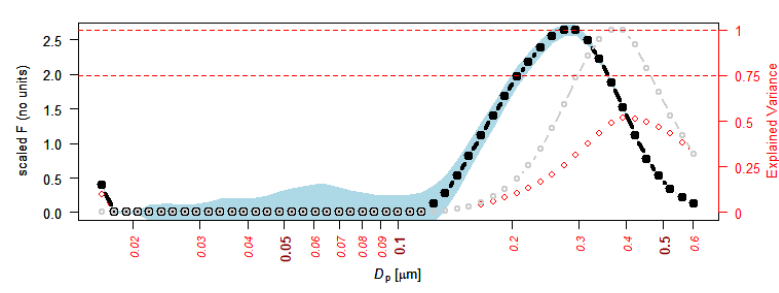
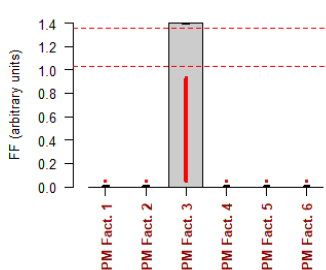
Diffuse Urban

2F_4



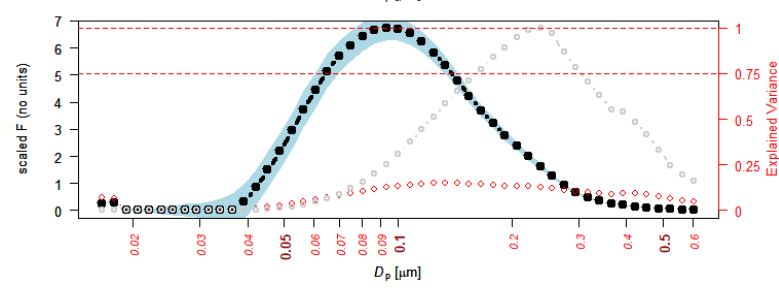
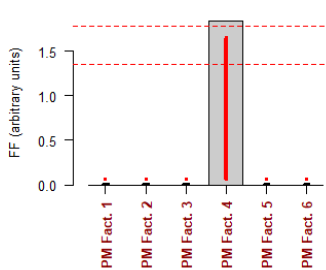
Marine

2F_2



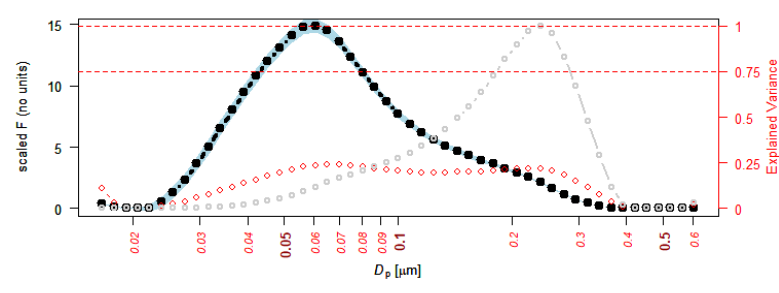
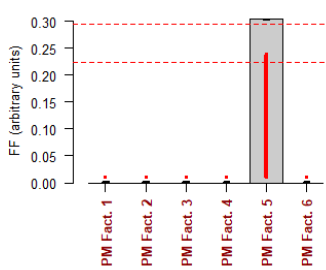
Secondary

2F_3



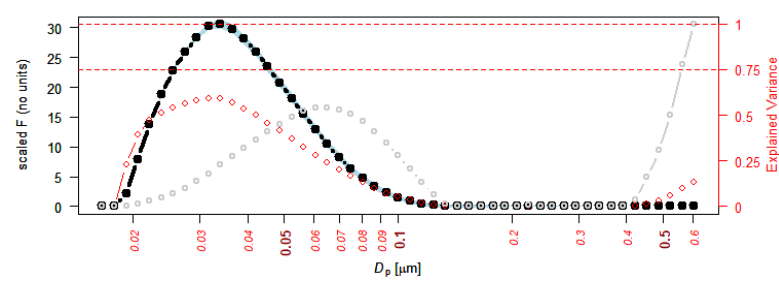
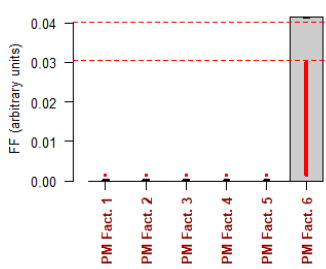
NET & Coarse

2F_4



Fuel Oil

2F_5



Traffic

2F_6

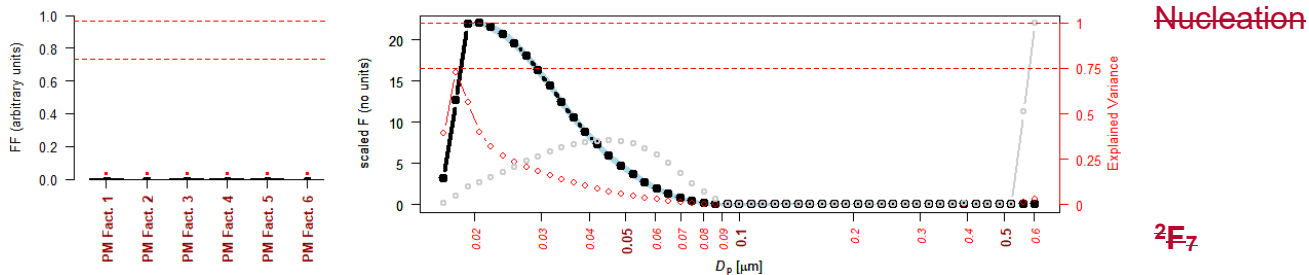


Figure S4. Source profiles 1F and 2F from both the first and second PMF step using 7 factors. [Grey bars and black line indicates the values of F ; red lines and dots indicated the explained variation; and grey dotted line indicates the $dV/d\log D_p$.]

72
73
74
75

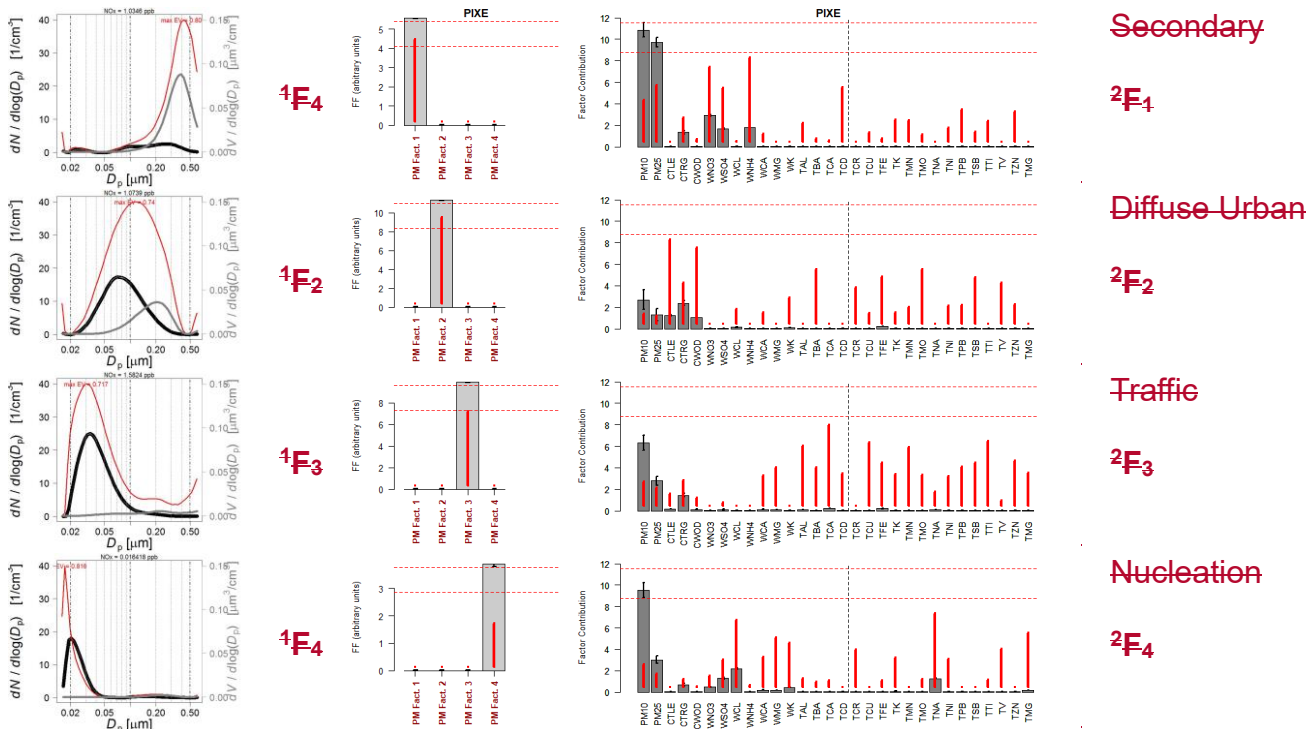


Figure S5. PMF-PMF 4 factor analysis of NSD data followed by PM_{10} . Each plot is divided into 2 showing the output 1F_k and 2F_k . [Grey bars and black line indicates the values of F ; red lines and dots indicated the explained variation; and grey dotted line indicates the $dV/d\log D_p$.]

76
77
78
79
80
81
82
83